CHEMISTRY OF MATERIALS
Review

*Chem. Mater.* **2010,** *22,* 675–690 675
DOI:10.1021/cm902687z

# New Chemical Systems for Solid Oxide Fuel Cells†

A. Orera and P. R. Slater*

*School of Chemistry, University of Birmingham, Birmingham, B15 2TT, U. K.*

*Received August 31, 2009*

In this review article, new systems being investigated for application in solid oxide fuel cells are discussed. For the electrode materials, materials with the perovskite or related structures continue to dominate the field, due to the need for high electronic conductivity. Research in this field is being directed toward compositions allowing high ionic conductivity in addition to their electronic contribution. In contrast, research on new electrolyte materials has shown a diverse range of structure-types, with an apparent tendency toward structures containing cations in lower coordination environments, particularly tetrahedral. In both the electrode and electrolyte area, materials allowing the incorporation of oxygen excess into interstitial sites have shown promising results, warranting further investigations of materials that will allow this type of defect chemistry.

## 1. Introduction

With the growing concerns regarding increasing greenhouse gas emissions and diminishing fuel reserves, research on fuel cell technologies has risen to high prominence both from the academic and industrial communities. Fuel cells are electrochemical power generation devices, which offer higher efficiencies than conventional power production based on combustion processes. They have a wide range of potential applications ranging from providing power for portable devices (e.g., mobile phones, laptop computers) and transport applications, to both small and large scale stationary power applications. In terms of the latter, solid oxide fuel cells offer the greatest prospects for commercialization, with a number of companies in this area developing systems for the market. Solid oxide fuel cells (SOFCs) are all solid state systems consisting of three main components, an electrolyte (which conducts oxide ions or protons), a cathode, and an anode. They operate at elevated temperature (500−1000 °C) to ensure adequate ionic conduction in the electrolyte, and electrical output is obtained when fuel is provided to the anode side of the cell, with air (oxygen) provided to the cathode. The high temperature operation offers both benefits and disadvantages, compared to other lower temperature fuel cells (e.g., polymer). In terms of the benefits, it allows the use of a wide range of fuels (from hydrogen to hydrocarbons), along with cheaper (nonprecious metal) materials for the electrodes. However, the key disadvantages are in terms of the difficulty in maintaining sealing of the cells (particularly for temperatures >700 °C), long-term stability of the individual materials, and compatibility (both chemical and thermal) between electrolyte and electrodes. As a result, there has been huge interest in the development of new materials with improved performance for potential use in future SOFCs, and this review will highlight some of the most interesting new systems. In the rest of this introduction, an outline of the conventional materials that have attracted interest for potential use in SOFCs will be presented, with sections 2−4 discussing the new materials.

**1.1. Conventional Electrolytes.** Those materials with applicability as electrolytes in a fuel cell must have a wide range of characteristics, including high ionic conductivity (oxide ion or proton), high ionic transport numbers (negligible electronic conductivity) in a wide range of oxygen partial pressures, chemical stability at high temperatures under partially reducing/oxidizing conditions, and good sinterability for their fabrication as gastight membranes with very thin thicknesses.[1] In traditional oxide ion conductors, the ionic transport mechanism is mediated by the presence of oxygen vacancies, and the materials most widely studied are fluorite- or perovskite-related, which allow the formation of these extrinsic anion vacancies by aliovalent doping.[2]

Stabilized zirconia, which has the fluorite structure (Figure 1), was first used in a fuel cell[3] in 1937, although it had previously been employed as the electrolyte in the Nerst-lamp. In modern fuel cells, the tetragonal/cubic form is stabilized by producing a solid solution with trivalent rare earths $ZrO_2-Ln_2O_3$ or divalent alkaline earth metals $ZrO_2-AO$. The most widely used are those stabilized with yttrium (YSZ) or scandium[4] (SSZ). The conductivities of these solid solutions increase with the degree of substitution to an optimum for 8% $Y_2O_3$ and 11% $Sc_2O_3$,[5] and this maximum conductivity is reached at a degree of substitution close to the minimum that stabilizes the cubic fluorite phase.[6,7] The highest ionic conductivities are found by doping with scandium,[8] although such systems have higher cost than the

† Accepted as part of the 2010 "Materials Chemistry of Energy Conversion Special Issue".

*Corresponding author. Tel.: +44 (0)121 4148906. Fax: +44 (0)121 4144403. E-mail: p.r.slater@bham.ac.uk.


Published on Web 11/05/2009

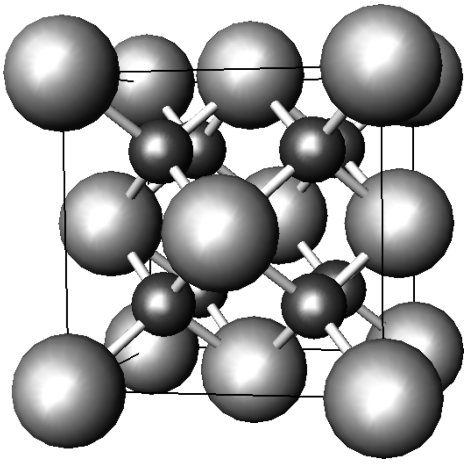

**Figure 1.** Fluorite structure adopted by $ZrO_2$ and $CeO_2$ (large spheres = Zr/Ce, small spheres = O).

corresponding $Y_2O_3$ doped systems. Consequently, YSZ has become the electrolyte most widely used in SOFCs. It has excellent properties as an electrolyte, although one major drawback is that high working temperatures (800−1000 °C, depending on the thickness of the electrolyte) are needed to obtain sufficient ionic conductivity, with the consequent problems with high temperature sealing and of compatibility with the rest of the materials used in the fuel cell.

The drawback of high working temperatures can be partially overcome by replacing YSZ with a stabilized ceria, which has higher conductivities than YSZ, allowing for lower temperature operation (500−700 °C).[9−11] Stabilized ceria is normally doped with gadolinia (CGO) or samaria (SDC) for the creation of the oxygen vacancies required to deliver high oxide ion conductivities.[12−14] The optimum doping levels are in this case close to 10−11% of rare earth oxide.[15] The main drawback of stabilized ceria is the partial reduction of $Ce^{4+}$ to $Ce^{3+}$ under the high temperature reducing conditions present in a fuel cell, which leads to electronic *n*-type conductivity and thus a decrease in the performance of the cell. However, the reduction of cerium has been shown to be almost negligible at temperatures below 600 °C, and so stabilized ceria is a suitable candidate for intermediate temperature fuel cells (500−600 °C), with the commercialization of such cells being investigated.

Recently, a very interesting observation has been made by Kim et al., who have observed power generation in water concentration cells at room temperature using YSZ or SDC electrolytes when they are nanostructured.[16,17] This result is based on the previous discovery of ionic conductivity at low temperature in YSZ when the grain size is ≈15 nm[18] and, although the power density obtained is at present very low and needs further optimization, it opens up a very exciting prospect of study inside the field of nanoionics.[19−22]

Bismuth based fluorite systems have also attracted considerable attention, although potential SOFC applications in these cases are limited. Nevertheless, it is useful to mention them here to highlight the problems that can be faced when developing a SOFC electrolyte. The high temperature phase $\delta$-$Bi_2O_3$ shows the highest oxide ion conductivity reported for a solid electrolyte due to its intrinsic oxygen vacancies, with one in four anion sites vacant.[23,24] The transition to the fcc $\delta$-$Bi_2O_3$ occurs between 705 and 730 °C. This variation in temperature depends mainly on the purity of the samples, their thermal prehistory, and their oxygen stoichiometry.[25] The stabilization[26] of this high temperature phase to room temperature has been made by doping with rare earth elements[27−29,31,32] obtaining conductivity values of $1.3 \times 10^{-2}$ S $cm^{-1}$ at 500 °C. Some studies claim that these $Ln_2O_3$-stabilized fcc phases are metastable[33] and need the use of double stabilizers, for example codoping with other metals such as Nb and W.[34−38] For example, $(Bi_2O_3)_{0.735}(Er_2O_3)_{0.21}(WO_3)_{0.055}$ shows a conductivity of 0.05 S $cm^{-1}$ at 550 °C[33] while $(BiO_{1.5})_{0.88}(DyO_{1.5})_{0.08}(WO_3)_{0.04}$ has a conductivity of 0.043 $cm^{-1}$ at 500 °C. This codoping also increases the stability of the material with time.[39] These high conductivities should offer this material huge potential as an SOFC electrolyte; however, in reality these materials have major drawbacks, including partial reduction under low oxygen partial pressures, bismuth volatility at relatively low temperatures, high thermal expansion coefficients, and poor mechanical properties.[40,41] Consequently, they are of limited use as SOFC electrolytes, and this highlights the problems faced when developing new materials; i.e., it is not just the high ionic conductivity that is needed.

In terms of other fluorite-related materials, there have been some studies into materials with the pyrochlore structure $A_2B_2O_7$,[42,43] which can be considered as a superstructure of a defective fluorite $(A,B)O_2$ with one anionic vacancy per formula unit. The main difference with the ideal fluorite is the additional ordering in the cation and anion sublattices present in the pyrochlore structure. The partial loss of this ordering is a key point for ensuring the high ionic conductivity of these materials. One of the systems most widely studied is $Gd_2(Ti_{1-x}Zr_x)_2O_7$,[44,45] which shows a large increase in conductivity with increasing $x$ due to structural disorder. $Gd_{2-y}Ln_yZr_2O_7$ solid solutions (Ln = Sm, Nd, and La) are also good ionic conductors.[46] Significant proton conductivity has been reported for some pyrochlore systems, especially for $La_2Zr_2O_7$-based systems, where proton incorporation is promoted by doping with lower valent cations on the A- or B-sites.[47] Higher proton conductivities are found for zirconates doped on the A-site, i.e. the proton conductivity of $(La_{1.95}Ca_{0.05})Zr_2O_{7-\delta}$ is $6.8 \times 10^{-4}$ S $cm^{-1}$ at 600 °C; three times larger than that of the system doped on the B site, suggesting differences in the proton concentrations.[48−51] However, the total ionic conductivities found for these materials are still below the values obtained for YSZ and CGO, and so, their applicability in solid oxide fuel cells remains limited.

Perovskite materials (Figure 2) have also been the subject of a great deal of research for SOFC electrolyte applications. High oxide ion conductivity was reported in 1994 simultaneously by Goodenough[52] and Ishihara[53] in

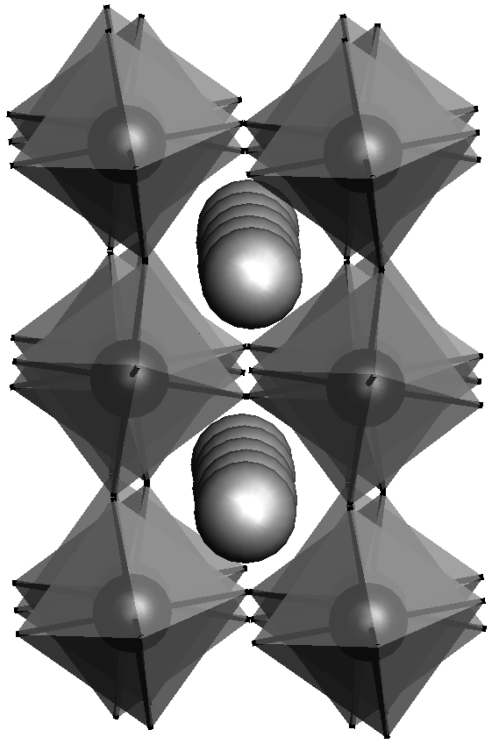

**Figure 2.** Perovskite structure adopted by $LaGaO_3$ (octahedra = $GaO_6$, large spheres = La).

substituted lanthanum gallate systems of composition $La_{1-x}Sr_xGa_yMg_{1-y}O_{3-\delta}$ (LSGM). The conductivity of the lanthanum gallate system is increased by codoping on both the La and Ga site to produce the requisite oxide ion vacancies. Although $Mg^{2+}$ is the main dopant on the Ga site, with typically $y = 0.15-0.2$, small codoping with Co, Fe, and Ni[54,55] seems to have beneficial effects on the conducting properties. For example, the introduction of small amounts of Co ($La_{0.8}Sr_{0.2}Ga_{0.8}Mg_{0.115}Co_{0.085}O_3$) increases the oxide ion conductivity, especially at low temperatures (0.1 S $cm^{-1}$ at 650 °C), without causing problems of increasing the *p*-type electronic conduction significantly.[56,57] With conductivities similar to those of SSZ allowing lower operation temperatures, these perovskite have a lot of potential for SOFC applications, although their main drawbacks are the volatility of Ga at high temperature under reducing conditions and the reactivity with Ni, present in the most commonly used anodes. However, they do have the advantage of a better stability, with regards to their ionic transport number, at low $pO_2$ than stabilized ceria.

While doped $LaGaO_3$ is an excellent oxide ion conductor, other perovskite materials originally conceived as oxide ion conductors have been confirmed to be good proton conductors as well.[58,59] In general, water dissolves in the acceptor-doped oxides filling the oxygen vacancies according to eq 1.

$$H_2O + V_O^{\bullet\bullet} + O_O \leftrightarrow 2OH_O^{\bullet} \quad (1)$$

However, although the most favorable site for the interstitial proton is linked to a lattice oxygen creating a hydroxide anion, the hydrogen transport is mediated by free proton migration (Grotthus mechanism) and not by a vehicle mechanism of hydroxide ion transport.[60−62] The most widely studied perovskite proton conducting systems are cerates[63,64] and zirconates[65] in the form $Ba(Zr/Ce)_{1-x}Y_xO_{3-x/2}$. The cerates are the systems with higher proton conductivity, but show problems of stability versus $CO_2$. Doped barium zirconate has the advantage of having higher chemical stability but presents some problems of poor sinterability and poorly conducting grain boundaries.[66] There have, however, been some recent advances in respect of these problems. Zn doping (< 5%) in these systems has been shown to be successful in allowing densification (> 95% theoretical) at temperatures of 1200 °C, which is about 200 °C lower than without Zn doping.[67,68] In addition, these Zn doped dense membranes were shown to display relatively good stability in $CO_2$ atmospheres.

High proton conductivity has also been reported for complex perovskites of the type $A_2(B'B'')O_6$ and $A_3(B'B_2'')O_9$, where A is a divalent cation, B′ is a divalent or trivalent cation respectively and B″ is a pentavalent metal, usually Nb or Ta.[69,70] To attain this high conductivity, it is necessary to produce oxide ion vacancies, which is achieved by increasing the concentration of the B′ ions at the expense of the B″ ions. Some examples include $A_3Ca_{1+x}Nb_{2-x}O_{9-3x/2}$,[71] $Sr_3CaZr_{0.5}Ta_{1.5}O_{8.75}$,[72] or $Sr_2Sc_{1+x}Nb_{1-x}O_{6-x}$.

Brownmillerite-type $Ba_2In_2O_5$ has also attracted considerable interest. This phase can be classed as an oxygen defective perovskite, where at room temperature the oxygen vacancies are ordered, resulting in alternating layers of octahedral and tetrahedral indium.[73,74] This phase then undergoes an order/disorder transition to a tetragonal perovskite above 900 °C that gives a drastic increase in its oxide ion conductivity (0.1 S $cm^{-1}$ at 900 °C). Several doping strategies have been suggested for lowering the temperature of this transition or even suppressing it, for example substitutions on the In site by W,[75] Ti,[76] Ga,[77,78] V, Mo,[79] or on the Ba site by La[80,81] or Sr.[82] Doping on the In site with a more stable trivalent metal also improves the stability against $CO_2$ and reduces the problem of volatilization of $In_2O_3$.[83] Proton conductivity has also been reported in these materials.[84,85]

Overall in terms of these conventional electrolytes, the $ZrO_2$ and $CeO_2$ based electrolytes have dominated in industrial devices, although $LaGaO_3$ and $BaCeO_3$ based systems show significant promise.

**1.2. Conventional Anodes.** In a solid oxide fuel cell, the oxidation of the fuel (hydrogen or hydrocarbons) takes place at the anode. The materials used for the fabrication of this electrode therefore need to accomplish a series of requirements of electrocatalytic activity for this reaction and stability in severely reducing environments, together with high electronic conductivity and compatibility with the rest of the materials of the SOFC system. Traditionally, the most widely used anodes for SOFCs consist of a metallic component dispersed into a matrix of the electrolyte material. These cermets are designed to accomplish the requirements of high electronic conductivity,

electrocatalysis, and appropriate microstructure, while minimizing problems due to coking and sulfur poisoning reactions. As a result of its electrochemical activity in hydrogen oxidation and hydrocarbon reforming, nickel is the preferred metal in these cermets.[86] Its mixture with the electrolyte material favors the thermomechanical matching with the electrolyte, while at the same time avoiding the formation of Ni agglomerates that would reduce the surface area and hence the amount of triple phase boundaries necessary for the catalytic processes.

In the YSZ based SOFC, the anode is usually a Ni/YSZ composite[87] with 40−60% Ni. These materials are normally produced from NiO/YSZ mixtures that are reduced in situ to obtain Ni metal. However, Ni based anodes do have some drawbacks, such as their reactivity with some La containing electrolytes,[88] as well as more critically their low tolerance to sulfur (present in significant quantities in natural gas) and the deposition of carbon (coking) when hydrocarbons are used as the fuel and the steam levels are low.[89,90] The stability and performance of the anode toward hydrocarbon fuels can be improved when CGO is used instead of YSZ, the ceria providing additional catalytic activity.[91] In addition, the activity of the Ni-based cermets for hydrogen oxidation also increases when ceria is used as a matrix in the order Ni/YSZ < Ni/$CeO_2$ < Ni/SDC < Ni/PrOx.[92] Copper has also been proposed as an alternative to Ni,[93−95] although $CeO_2$ is typically added to provide the requisite catalytic activity. However, a recent study has shown the destabilization of YSZ in the presence of copper compounds, which leads to the formation of monoclinic zirconia.[96] Finally, another important drawback of the use of these cermets as anodes is their poor redox stability due to the change in volume that they show when exposed to oxidation processes, which leads to the degradation of the cell and decrease in performance.[97]

**1.3. Conventional Cathodes.** Apart from the general stability and compatibility requirements of any fuel cell material, those used in the cathode electrode need to have high electronic conductivity under oxidizing conditions and a good catalytic activity toward promoting oxygen dissociation. Most of the traditionally used cathodes have the perovskite structure, e.g. doped $LaMnO_3$ and $LaCoO_3$,[98] and typically, they are employed as a composite with the electrolyte. A detailed compilation of perovskite materials for cathode applications can be found in a comprehensive review by Skinner.[99] In lanthanum manganate $LaMnO_3$, the high *p*-type electronic conductivity arises from the presence of mixed valence Mn ($Mn^{3+}$ and $Mn^{4+}$), which is enhanced by doping with alkaline earths, especially Sr.[100,101] $La_{1-x}Sr_xMnO_3$ (LSM) has very good electronic conductivity at high temperature, but possesses poor oxide ion conductivity. In addition, it reacts with YSZ electrolytes at high operating temperatures forming an insulating interface that decreases the performance of the cell, especially when large Sr/La ratios are used. The analogous cobalt phase $La_{1-x}Sr_xCoO_3$ (LSC)[102] improves the cathode performance, especially when CGO is used as the electrolyte,[103,104] by increasing the catalytic activity and oxide ion conductivity. However, this material also reacts with YSZ electrolytes, and its thermal expansion coefficient (TEC) ($\approx 23 \times 10^{-6}$ $K^{-1}$) is much higher than that of YSZ and other typical SOFC electrolytes. The use of composites with the electrolyte can, however, help to partially overcome this mismatch. Zhao et al.[105] have recently reported the preparation of composites of LSC with $Sm_{0.2}Ce_{0.8}O_{1.9}$, with good performance and high resistance to thermal cycles and thermal shock observed. Further investigation on the stability of these cobaltate systems and their use at low temperatures has pointed to other compositions as promising, e.g. $Gd_{1-x}Sr_xCoO_3$ and $Sm_{1-x}Sr_xCoO_3$.[106,107] Doping with Fe on the Co site in $La_{1-x}Sr_xCo_{1-y}Fe_yO_{3-\delta}$ (LSCF) has also attracted interest, leading to a better thermal expansion coefficient match, and improved stability at high temperature.[108,109]

## 2. New Cathode Materials

In the search for new SOFC cathode materials, the need for high electronic conductivity, along with ideally high ionic conductivity has meant that perovskite and related (e.g., Ruddlesden−Popper) systems have dominated the research.

**2.1. Ruddlesden−Popper-type Materials.** Ruddlesden−Popper-type materials have emerged in recent years as promising alternatives to the traditional perovskites for use as cathodes in SOFCs. These systems have the general formula $A_{n+1}M_nO_{3n+1}$ (A = rare earth/alkaline earth; M = transition metal) and consist of perovskite layers separated by rock salt layers, the value of *n* determining the perovskite layer "thickness". They show a diverse defect chemistry, allowing both hypo- and hyperstoichiometry in terms of their oxygen content, which makes them very attractive for the fine-tuning of their electrical properties. In particular, oxygen hyperstoichiometry can be achieved through the incorporation of excess oxide ions into interstitial sites within the rock salt layers. The most widely studied systems are the $n = 1$ phases, which possess the well-known $K_2NiF_4$ structure (Figure 3)[110−115] with the greatest emphasis on the $La_2NiO_{4+\delta}$ composition. Despite promising cathode electrochemical properties, they still present some problems in terms of compatibility with the electrolyte. For example, Sayers et al.[116] have studied their applicability in the intermediate temperature range by analyzing the compatibility of $La_2NiO_{4+\delta}$ with CGO and LSGM as electrolytes. The results showed significant reactivity of $La_2NiO_{4+\delta}$ with CGO after heating at 900 °C, and thus, its application with this electrolyte may require the use of a protective layer between electrolyte and electrode. In contrast, no signs of reaction were found between $La_2NiO_{4+\delta}$ and LSGM, although other studies have suggested some reactivity.[117] Tests of $La_2NiO_{4+\delta}$ electrodes in symmetrical cells with CGO electrolyte gave an area specific resistivity (ASR) of 3.4 Ω $cm^{-2}$ at 640 °C, with similar results also observed when YSZ is used as the electrolyte.[118] $La_2NiO_{4+\delta}$ has also been found to react with some of the newer electrolytes, which will be discussed in the next section.

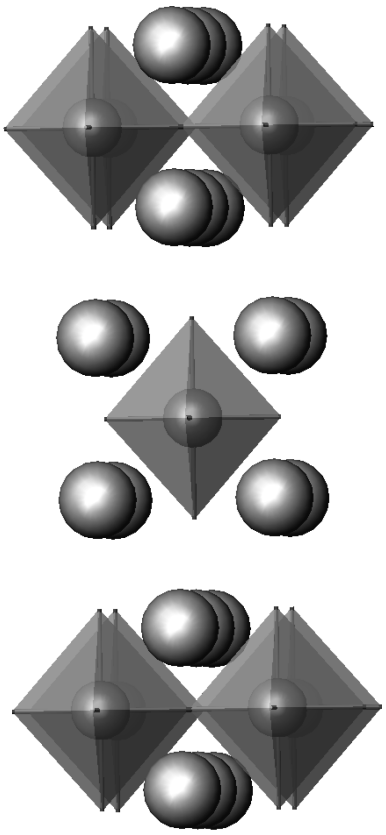

**Figure 3.** $K_2NiF_4$ structure adopted by $La_2NiO_4$ (octahedra = $NiO_6$, large spheres = La).

There have been a wide range of fundamental studies into this material with the influence of the thickness of the $La_2NiO_{4+\delta}$ layers having been studied by various authors,[119,120] in addition to the effect of multilayer ceramics combining dense and porous components.[121] From a chemical point of view, however, the most interesting studies have concerned the optimization of this system through La and/or Ni site substitution. Regarding the Ni site substitutions, the cations most commonly examined have been Co,[122] Fe,[123,124] and Cu. Recently, Aguadero et al.[125] have evaluated the performance of materials from the series $La_2Ni_{1-x}Cu_xO_{4+\delta}$ on both YSZ and LSGM electrolytes, finding the lowest ASR values with LSGM as electrolyte. Cu-substituted samples were reported to exhibit lower ASR than undoped $La_2NiO_{4+\delta}$, with the best performance observed for intermediate compositions ($x = 0.4$). Zhao et al.[126] have examined the introduction of high levels of Co along with codoping with Sr, $La_{2-x}Sr_xCo_{0.8}Ni_{0.2}O_{4+\delta}$ ($x = 0$, 0.4, 0.8, 1.2, 1.6). Cathode composites of these materials with $Ce_{0.9}Gd_{0.1}O_{1.95}$ were produced, with the best performance observed for $x = 0.8$. $LaSrFeO_{4+\delta}$ materials[127] have also been examined and reported to show similar electrochemical performance to that of nickel based systems.

The partial substitution of La by Sr in $La_2NiO_{4+\delta}$ has also been widely studied, with recent steady-state oxygen permeation measurements for $La_{1.9}Sr_{0.1}NiO_{4+\delta}$[128] in comparison to $La_2NiO_{4+\delta}$[129] showing that the former has a higher activation energy for the oxygen self-diffusion coefficient ($D_O$) and similar activation energy for the surface-exchange coefficient. The lower values of $D_O$ in $La_{1.9}Sr_{0.1}NiO_{4+\delta}$ can be correlated with the lower concentration of oxygen interstitials ($\delta$), showing the importance of these.

Further doping studies have examined varying the rare earth cation, and Mauvy et al. have reported lower cathodic ASR values for praseodymium nickelate, $Pr_2NiO_{4+\delta}$.[130] The effect of doping on the Ni site in $Pr_2NiO_{4+\delta}$ was studied by Miyoshi et al.,[131] who reported that the oxygen permeation rate was improved by doping with Cu and Mg. Neodymium nickelates have also been investigated, with reports suggesting that these show improved chemical stability versus CGO[132] and YSZ,[130] since no reaction was found when using $Nd_{2-x}Sr_xNiO_4$ and $Nd_{1.95}NiO_{4+\delta}$, respectively, as electrodes.

As noted at the start of this section, one of the most interesting features of these systems is their ability not only to accommodate oxide ion vacancies, as for perovskite cathodes, but also to allow the introduction of oxide ions into interstitial sites. An important feature is therefore an understanding of the influence of composition on the ionic transport mechanism. The diffusion path of oxide ions in $(Pr_{0.9}La_{0.1})_2(Ni_{0.74}Cu_{0.21}Ga_{0.05})O_{4+\delta}$ has been reported from a high-temperature neutron powder diffraction study.[133] The results showed that the oxygen atom at the O2 site (0 0 $z$) exhibits highly anisotropic thermal motion ($U_{11} = U_{22} > U_{33}$), which leads to the migration of oxide ions to the nearest-neighbor interstitial O3 positions, forming curved O2−O3 diffusion paths in a 2D arrangement. This anisotropy is also corroborated by Burriel et al.,[134] who determined the anisotropic oxygen tracer diffusion and surface exchange coefficients in epitaxial thin films. They showed that both coefficients are two to 3 orders of magnitude lower along the *c*-axis than in the *ab* plane. Atomistic computer simulations carried out by Cleave et al.[135] have also predicted this anisotropy, with calculated activation energies of 0.35 eV for the vacancy migration in the *ab* plane compared to 0.77 eV along the *c*-axis. In addition, this work predicted the interstitial migration in the *ab* plane to have an energy barrier of 0.86 eV, suggesting a vacancy conduction mechanism be favored. An in situ high temperature neutron powder diffraction study has also been carried out on $La_2Ni_{0.6}Cu_{0.4}O_{4+\delta}$[136] to explain the change in the conduction regime from semiconductor-like below 400 °C to high-temperature metallic behavior. The authors correlated this change in regime with an abrupt contraction in the axial Ni−O2 bond lengths at 400 °C, causing the shrinkage of the perovskite layer along the *c* direction.

Apart from the $K_2NiF_4$-type materials, higher-order ($n > 1$) Ruddlesden−Popper phases have also been studied as cathodes for SOFCs. Amow and Skinner[113] prepared $La_{n+1}Ni_nO_{3n+1}$ ($n = 2$ and 3) phases, which were obtained as the anion deficient $La_3Ni_2O_{7-\delta}$ and $La_4Ni_3O_{10-\delta}$, respectively; the higher Ni oxidation state ($n = 1$, 2+; $n = 2$, 2.5+; $n = 3$, 2.67+) in the stoichiometric phase for these higher order systems meaning that oxide ion vacancies

rather than interstitials predominate to lower this valence.[137−139] Despite these different defect characteristics, these materials showed improved thermal stability, electrical conductivity, and electrode performance over that of $La_2NiO_{4+\delta}$. The synthesis of these materials was later improved by a single-step heat treatment of nanosized metal hydroxide cocrystallized precursors.[140]

**2.2. Layered Double Perovskites.** Despite the growing interest in Ruddlesden−Popper type systems, perovskite materials continue to attract the most attention as cathodes, with significant interest in the double perovskites, $AA'B_2O_{6-\delta}$, where A′ is normally Ba, A is a lanthanide, and B is a first row transition metal. The most widely studied compositions correspond to the $LnBaCo_2O_{5+\delta}$ formula, with Ln = Pr, Nd, Sm, Gd.[141−144] The key feature of these materials is that A and A′ are ordered in alternate layers, and two features make them attractive for application as cathode materials: their high electronic conductivity above the metal−insulator transition temperature (around 350 °C) and their excellent oxide ion conductivity.[145,146] The oxide ion mobility appears to increase with increasing ionic radius of the $Ln^{3+}$ cation, since the large lanthanides increase the nominal oxidation state of the cobalt ions and hence the oxygen content.[147] Thus, $PrBaCo_2O_{5+\delta}$ shows very good oxygen transport properties along with very fast oxygen surface exchange kinetics.[148,149] However, although the oxygen permeation flux for $PrBaCo_2O_{5+\delta}$ is higher than that of $GdBaCo_2O_{5+\delta}$ ($8.0 \times 10^{-8}$ mol cm$^{-2}$ s$^{-1}$ compared to $2.6 \times 10^{-8}$ mol cm$^{-2}$ s$^{-1}$ at 800 °C), the activation energy is also much higher (134.9−49.1 kJ mol$^{-1}$), and as a result, when the temperature decreases below 675 °C, the oxygen permeation flux of $PrBaCo_2O_{5+\delta}$ is smaller than that of $GdBaCo_2O_{5+\delta}$.[150]

Tarancón et al.[151] have reported very promising results for $GdBaCo_2O_{5+\delta}$[152] tested in symmetrical cells with $La_{0.8}Sr_{0.2}Ga_{0.8}Mg_{0.2}O_{3-\delta}$ and $Ce_{0.9}Gd_{0.1}O_{1.95}$ electrolytes, obtaining ASR as low as 0.25 Ω cm$^2$ at 625 °C. However, high reactivity was found with YSZ at temperatures as low as 700 °C. Peña-Martinez[153] have compared $GdBaCo_2O_{5+\delta}$ and the related perovskite $Ba_{0.5}Sr_{0.5}Co_{0.8}Fe_{0.2}O_{3-\delta}$ as cathodes on $La_{0.9}A_{0.1}Ga_{0.8}Mg_{0.2}O_{2.85}$ (A = Sr, Ba) electrolytes, finding that the performance of both cathode materials was better when Sr was used in the electrolyte, with lower ASR values for $Ba_{0.5}Sr_{0.5}Co_{0.8}Fe_{0.2}O_{3-\delta}$ in the 600−800 °C temperature range. This latter phase will be discussed in more detail in the next section.

When the lanthanide used is Pr, ASR values as low as 0.4 Ω cm$^2$ were measured at 600 °C in air, based on symmetric cell tests.[154] A thin-film SDC electrolyte fuel cell with a $PrBaCo_2O_{5+\delta}$ cathode delivered good peak power densities of 620 and 165 mW cm$^{-2}$ at 600 and 450 °C, respectively. Promising results have also been reported for analogous materials with Sm as the rare earth cation. A $SmBaCo_2O_{5+\delta}$ cathode on SDC and LSGM electrolytes gave polarization resistances of 0.098 and 0.054 Ω cm$^2$, respectively, at 750 °C,[155] with maximum power densities for a single cell reaching 641 and 777 mW cm$^{-2}$, respectively, at 800 °C. The low temperature synthesis of this $SmBaCo_2O_{5+\delta}$ material has been reported by Sun et al.,[156] who successfully synthesized it by the citric acid−nitrate gel combustion process at temperatures as low as 900 °C for 4 h, using undissolved and relatively inexpensive $Co_3O_4$ as a starting material. Through such low temperature synthesis routes, control of particle size and hence cathode morphology can be achieved, hence offering further advances.

Apart from the layered cobaltates, layered cuprates $LnBaCuMO_{5+\delta}$ (M = Fe, Co) have also been studied as potential cathode materials for intermediate temperature SOFCs. Zhou et al.[157] have studied the applicability of $LaBaCuFeO_{5+x}$ and $LaBaCuCoO_{5+x}$ as cathodes in combination with SDC electrolytes. They reported ASR values of 0.21 and 0.11 Ω cm$^2$, respectively, at 700 °C. However, the chemical and long-term stability of these compounds still needs to be evaluated.

**2.3. Other Perovskite Materials.** $Ba_{0.5}Sr_{0.5}Co_{0.8}Fe_{0.2}O_{3-\delta}$ (BSCF) has become a very promising cathode material to allow lower temperature operation. This was first reported as a potential IT-SOFC cathode material for samarium doped ceria electrolytes by Shao,[158,159] and a recent review by Zhou et al.[160] highlights the existing interest on the understanding and development of this cathode system. Baumann et al.[161] have recently tested the electrochemical properties of BSCF with thin film microelectrode configuration, finding extremely low surface exchange resistances, 50 times smaller that that obtained for $(La,Sr)(Fe,Co)O_{3-\delta}$ materials. In agreement with this result, Wang et al.[162] have measured the oxide ion diffusion coefficient by means of SIMS finding high values, significantly larger than that for $(La,Sr)(Fe,Co)O_{3-\delta}$ perovskites. Further improvements in the conduction properties have been reported for rare earth substitutions, i.e. $(Ba_{0.5}Sr_{0.5})_{1-x}Ln_xCo_{0.8}Fe_{0.2}O_{3-\delta}$ with Ln = Sm,[163] Nd,[164] or La.[165] Although very high performances have been achieved with this cathode (1.3 W cm$^{-2}$ at 600 °C with GDC as electrolyte and a Ni-GDC cermet anode),[166] it also has some drawbacks. As with most of the Ba containing cathodes, it undergoes some surface carbonation in the presence of $CO_2$, to the detriment of the surface oxygen exchange coefficient and thus performance of the cell.[167,168] It also has some instability at low temperatures,[169] with decomposition occurring when the material is kept for long times at temperatures below 900 °C.[170]

Lanthanum nickel ferrite, $LaNi_{1-x}Fe_xO_3$ (LNF), has also been considered as an attractive material for use as a cathode, especially because of its high electronic conductivity, which reaches 580 S cm$^{-1}$ at 800 °C for $x = 0.4$.[171] Its thermal expansion coefficient is also suitable to match that of the YSZ, which favors the thermomechanical stability of the system. Another advantage of these LNF cathodes is their resistance against Cr poisoning, which can potentially diffuse from the cell interconnect material.[172] However, recent studies have claimed problems with its reactivity with YSZ and CGO forming poorly conducting phases at the electrolyte/cathode interface.[173,174] Doping with strontium on the lanthanum site, $La_{1-y}Sr_yFe_{1-x}Ni_xO_{3-\delta}$, has been reported to increase the

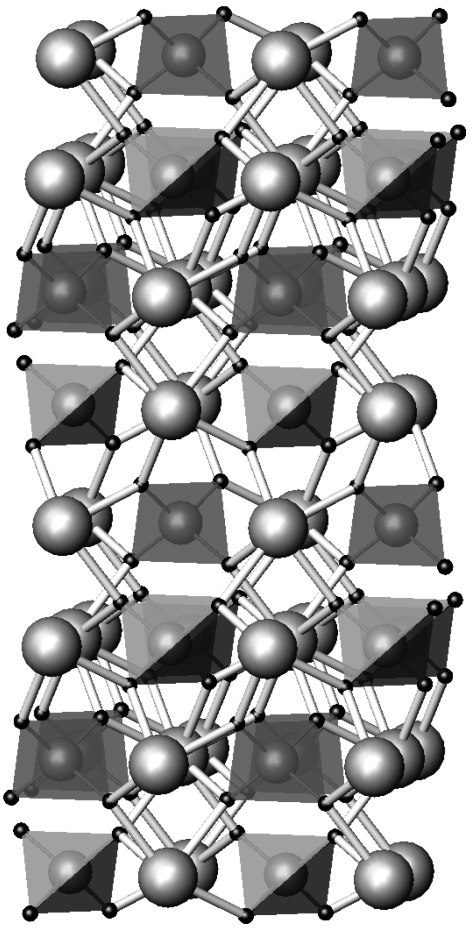

**Figure 4.** Structure of tetragonal $CeNbO_4$ (tetrahedra = $NbO_4$, large spheres = Ce).

ionic conductivity by the introduction of oxygen vacancies in the system but has the detrimental effect of increasing the thermal expansion coefficient. Cu doping in these systems has also been investigated, and fuel cells containing $LaNi_{0.2}Fe_{0.8-x}Cu_xO_3$ cathodes have been fabricated by Li et al.[175] The materials were prepared by the coprecipitation method, and single phase samples were obtained for $x < 0.15$. These fuel cells gave good peak power densities of 635 and 763 mW $cm^{-2}$ at 580 and 650 °C, respectively.

**2.4. Pyrochlore Materials.** Ru based electrodes have been suggested as promising candidates for low temperature SOFCs, due to their excellent catalytic activity toward oxygen reduction. In this respect, pyrochlore ruthenates, $A_2Ru_2O_7$ (A = Bi, Pb), have been studied as cathode materials, yielding low ASR values, although they do show stability problems. The chemical reactivity and long-term stability of these systems have been improved by preparing the solid solution $Bi_{2-x}M_xRu_2O_{7-\delta}$ (M = Sr, Pb)[176] with low $x$ values (Sr, $x = 0.1, 0.25$; Pb, $x = 0.5$). In addition, the use of composites seems to improve the performance of these pyrochlore materials. Camaratta et al.[177] have studied composite electrodes consisting of $Bi_2Ru_2O_7$ and $Er_{0.4}Bi_{1.6}O_3$, and by varying the weight percent of each phase in the composite and improving the microstructure, they obtained an area specific resistance of 0.03 Ω $cm^2$ at 700 °C. However, the high cost of these materials is still a major obstacle for their commercial development.

**2.5. Other Cathode Materials.** The mixed ionic/electronic conductor $CeNbO_{4+\delta}$ has recently been proposed as a potential cathode material. $CeNbO_{4+\delta}$ has the monoclinic fergusonite[178] structure at low temperatures, transforming to a tetragonal scheelite structure (Figure 4) at 750 °C.[179] As for the $K_2NiF_4$ materials discussed earlier, it has the ability to accommodate oxide ions in interstitial sites, and this ability to adopt different oxygen hyperstoichiometries ($0 \leq \delta \geq 0.33$) is particularly interesting.[180] The oxygen excess is achieved through partial oxidation of cerium, which also creates electron holes.[181,182] The applicability of this material as a cathode, however, depends at present on the need for further improvement in its electronic conductivity.

The spinel $Cu_{1.25}Mn_{1.75}O_4$ (CMO) has also been recently proposed[183] as a potential cathode for use with YSZ electrolytes. A cathode consisting of 50% CMO impregnated YSZ had a polarization resistance of 0.3 Ω $cm^{-2}$ at 750 °C.

## 3. New Oxide Ion Conducting Electrolytes

As detailed in section 1, there has been considerable interest in fluorite and perovskite oxide ion conductors, which have tended to dominate the SOFC field. As a result of the large amount of research on such electrolyte systems, the materials have essentially reached the state of the art that is possible. Consequently, in recent years, there has been a growing trend toward the investigation of alternative structure-types, for the prospect of future major advances. All these structure-types have been known for a considerable time but only through recent studies have they been shown to display high ionic conduction, highlighting the need for further rational investigation of the wide number of structure types known for identification of the next generation electrolytes.

**3.1. $La_2Mo_2O_9$.** $La_2Mo_2O_9$, first reported by Lacorre et al., shows very high conductivities (0.06 S $cm^{-1}$ at 800 °C), exceeding that of YSZ at elevated temperatures.[184] In their early work, Lacorre et al. showed that at low temperatures, the structure was likely monoclinic, and the oxide ion conductivity relatively low. At a temperature of ≈580 °C, a phase transition to a cubic cell was observed with an accompanying large jump in conductivity (nearly 2 orders of magnitude), reminiscent of that observed for the brownmillerite phase $Ba_2In_2O_5$. The monoclinic symmetry of the low temperature (α) form has since been confirmed by Evans et al.[185] This structural work showed that the material possesses a complex unit cell, containing variable coordination for Mo. PDF analysis of neutron diffraction data has indicated that the local structure is the same in both the low temperature (α) form and high temperature ($\beta$) form, indicating that the phase transition is related to a change from a static to a dynamic arrangement of oxide ion defects.[186] It is the presence of Mo with different coordination numbers, that is thought to be vital in ensuring the high conductivity,

with recent modeling work suggesting that the oxide ions move in a cooperative fashion.[187]

One of the problems with the undoped system is the fact that the conductivity only becomes practical for applications in the high temperature ($\beta$) form. Consequently, there has been a lot of interest in doping studies to stabilize the $\beta$ form to lower temperatures. This work has shown that most substitutions on either the La (e.g., other rare earths, alkaline earths, alkali metals, Bi) or Mo (e.g., W, V, S, Cr, Nb, Ta) sites will stabilize the cubic $\beta$ form, and enhance the low temperature conductivity.[184,188−197] In addition, F doping has also been shown to decrease the temperature of the order−disorder transition.[198] In terms of optimum dopants, most work has concentrated on rare earth and W doping. In particular, W doping helps to increase the stability of these systems in strongly reducing conditions, which is a significant concern for potential applications of these $La_2Mo_2O_9$ electrolytes. However high W levels also lead to a significant reduction in conductivity. In terms of a compromise between stability and conductivity, the composition $La_{1.7}Gd_{0.3}Mo_{0.8}W_{1.2}O_9$ has been reported to be most promising.[190] In addition, recently Nb doping has been shown to result in very high conductivities, higher than in the parent high temperature ($\beta$) form (0.11 S $cm^{-1}$ at 800 °C for $La_2Mo_{1.94}Nb_{0.06}O_{8.97}$).[191]

The very high oxide ion conductivity of these systems have been confirmed by isotope exchange depth profile techniques, where higher oxide ion diffusion coefficients ($1.4 \times 10^{-6}$ $cm^2$ $s^{-1}$ at 800 °C) than fluorite materials have been determined.[199] Despite these high oxide ion conductivities, this system is not without its problems, one being the stability in reducing conditions as highlighted above. In addition, Mo volatility is a concern at the high temperatures required to achieve dense membranes. Consequently, low temperature synthesis routes (e.g., spray pyrolysis, sol gel, combustion) to nanoparticulate materials have been examined, which have been successful in achieving dense membranes (>95% theoretical) at temperatures up to 300 °C lower than for powders prepared from conventional solid state reaction.[200,201] Another problem is the high reactivity with conventional SOFC cathode materials, attributed mainly to Mo diffusion into the cathode,[202] although the material has been shown to be stable in contact with NiO/Ni.[203] In addition, the material is also stable in conjunction with $CeO_2$ based electrolytes, and so, these have been explored as protective layers on the cathode side to avoid migration of Mo into the cathode.[204] However, such protective layers cannot overcome the problems of high thermal expansion displayed by this material ($15-20 \times 10^{-6}$ $K^{-1}$) in comparison to conventional fuel cell electrodes.[202]

Recently, there have been some interesting effects seen with regard to particle size and the production of thin films. Zhuang et al. have reported that the conductivity increases in $La_2Mo_{2-x}W_xO_9$ ($0 \le x \le 0.2$) with decreasing grain size in thin films.[205] Thus, a conductivity of 0.07 S $cm^{-1}$ was obtained at 600 °C for a sample with an average grain size of 90 nm.

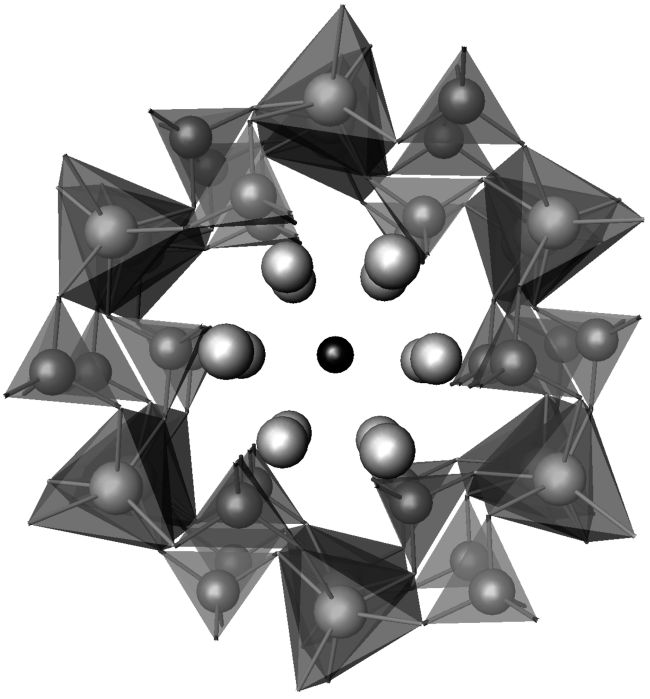

**Figure 5.** Apatite structure in terms of a $(A)_4(MO_4)_6$ framework (consisting of $AO_6$ trigonal metaprisms linked to $MO_4$ tetrahedra), with the remaining $A_6O_2$ units accommodated in the "cavities" within the framework.

Overall these materials are very promising oxide ion conductors, although the stability and thermal expansion mismatch problems outlined above are currently limiting SOFC applications.

**3.2. Apatite-type Materials.** Materials with the apatite structure have been widely researched internationally, although this work has traditionally mainly focused on their application as bioceramics, waste encapsulation materials, and as host structures for rare earth luminescence properties. Research into apatite materials as potential solid oxide fuel cell electrolytes was initiated by reports of very high oxide ion conductivity in lanthanide silicates with the apatite structure by Nakayama et al.[206,207] Subsequently, the germanium containing analogues were also identified as excellent oxide ion conductors.[208] Since these initial studies, work on these systems has grown significantly, although there is still a certain amount of confusion/controversy regarding their conduction mechanism, particularly for the silicate systems. Apatite-type oxides have an ideal general formula of $A_{10}(MO_4)_6O_2$, where A = alkaline earths, rare earths, M = Si, Ge, P. Their structure may be described as comprising of isolated $MO_4$ tetrahedra arranged so as to form distinct oxide ion and A cation channels running parallel to the *c* axis. More recently, White et al. have proposed an alternative description in terms of an $(A)_4(MO_4)_6$ framework, with the remaining $A_6O_2$ units accommodated in the "cavities" within the framework (Figure 5).[209] Both descriptions have their merits, with the latter White description being particularly useful in accounting for some of the crystallographic subtleties of these materials.

In terms of oxide ion conducting apatites, the best properties are observed for samples containing the lar ger rare earths (La, Pr, Nd) and M = Si, Ge, with no reports of high oxide ion conduction in M = P apatite materials.[210−222,222−227] In terms of the defects required for the high oxide ion conductivities, initially it was assumed that, as for the traditional fluorite and perovskite-type electrolytes, oxide ion vacancies were crucial, with a vacancy conduction mechanism proposed. However, subsequent work has identified the importance of interstitial oxide ions in these materials, the poor conductivities of apatites with M = P being attributed to their inability to accommodate interstitial oxide ions.[210,219,228] Thus, it has been shown that doping to introduce oxide ion excess, i.e. $La_{8+x}A_{2-x}(MO_4)_6O_{2+x/2}$ (A = Ca, Sr, Ba; M = Si, Ge), results in increasing oxide ion conductivity with values $> 1 \times 10^{-3}$ S cm$^{-1}$ at 500 °C for samples with high oxide excess ($x > 0.5$).[219] In addition to samples containing oxygen excess showing high oxide ion conductivity, there have also been reports of samples containing cation vacancies, but nominally stoichiometric in terms of oxygen, showing high conductivity, e.g. $La_{9.33}(SiO_4)_6O_2$. It has been proposed that the presence of cation vacancies causes local displacements which enhances Frenkel defect formation, and thus the conducting interstitial oxide ions are provided by intrinsic defects rather than extrinsic.[210,219]

The location of the interstitial sites within the structure in the silicate apatites, and the conduction mechanism for these silicates has attracted a considerable amount of discussion outside the scope of this review (for further details of the mechanisms proposed, see, for example, refs 219 and 228−232). However, an interesting observation is that conductivity measurements on single crystals have shown that although the conduction is anisotropic, being larger along the *c* direction, there is still substantial conduction perpendicular to the *c* direction (e.g., $\sigma_c = 1.3 \times 10^{-2}$ S cm$^{-1}$, $\sigma_{ab} = 1.2 \times 10^{-3}$ S cm$^{-1}$ at 500 °C for $Pr_{9.33}(SiO_4)_6O_2$[233]), and it has been proposed that "$S_N2$" type "exchange" processes are responsible for this latter conduction.[219] This is significant, as other structure-types, which have not been studied due to lack of perceived conduction pathways, may also display significant ionic conduction via similar processes, when suitably doped. In addition, the very high conductivities observed for single crystal samples along the *c* direction suggest that studies into orientated thin films are warranted.

Although there have been numerous reports in the literature of the synthesis of the composition $La_{10}(SiO_4)_6O_3$ (the $x = 2$ endmember of the $La_{8+x}A_{2-x}(SiO_4)_6O_{2+x/2}$ series), corresponding to an interstitial oxide ion content per formula unit of 1.0, such samples invariably contain $La_2SiO_5$, and so in terms of single phase samples, the maximum oxygen excess possible for the silicate series is closer to 0.5 per formula unit, e.g. $La_9A(SiO_4)_6O_{2.5}$ (A = Ca, Sr, Ba), $La_{9.67}(SiO_4)_6O_{2.5}$.[219] As noted earlier, the highest conductivities are observed for these samples with the highest oxygen excess. However, another strategy to improve the conductivity of these systems has been to dope on the Si site with lower valent cations, e.g. Mg, Ga, Al, Zn.[221,227,234−237] Mg doping on the Si site has been shown to be particularly beneficial, with conductivities as high as 0.074 S cm$^{-1}$ (at 800 °C) reported for $La_{9.8}(SiO_4)_{5.7}(MgO_4)_{0.3}O_{2.4}$.[238]

In contrast to the controversy regarding the location of the interstitial sites in the silicate systems, there appears to be greater concensus for the germanate apatites, with the interstitial oxide ions being reported to be adjacent to the $GeO_4$ tetrahedra, essentially resulting in the formation of five coordinate Ge.[209,224,239,240] As for the silicates, high conductivities are favored for samples containing high oxygen excess and/or the presence of cation vacancies. For these germanates, higher oxygen excess is achievable than for the corresponding silicates (up to 1.0 per formula unit). However, in this case, a further complexity arises in that on increasing the oxygen content, for the series $La_{9.33+x}(GeO_4)_6O_{2+3x/2}$ and $La_{8+x}A_{2-x}(GeO_4)_6O_{2+x/2}$, there is a change in symmetry from hexagonal to triclinic.[219] This results in a lower conductivity at low temperatures for such triclinic samples, e.g. $La_{10}(GeO_4)_6O_3$, attributed to additional defect trapping in the lower symmetry cell. This problem can be overcome through Y doping, e.g. $La_8Y_2(GeO_4)_6O_3$, which leads to hexagonal symmetry along with high conductivities.[219,240,241] As for the silicate apatites, Al doping on the Ge site has been reported to enhance the conductivity, with the highest conductivity in the literature reported for the composition, $La_{9.5}(GeO_4)_{5.5}(AlO_4)_{0.5}O_2$ (0.16 S cm$^{-1}$ at 800 °C).[211]

The apatite germanates tend to have higher activation energies than the corresponding silicates (≈1.0 eV versus 0.5−0.8 eV), and hence, the former show higher conductivities at elevated temperatures (> 800 °C), while the silicates have higher conductivities at lower temperatures.[219]

The work above therefore highlights the high oxide ion conductivities observed for these systems raising significant interest in terms of applications as SOFC electrolytes. In addition to their high conductivities, these apatites have compatible thermal expansion coefficients with current electrode materials, while the silicate apatites are also cheap systems in terms of raw materials (the germanates suffer from the high cost of $GeO_2$, although the flexibility of these apatite germanates to accommodate a range of dopants without a significant detrimental effect on the conductivity means that cheaper low purity $GeO_2$ could be employed). They can be readily produced by both conventional solid state and sol gel methods, with reports that ambient temperature synthesis through high energy ball milling is also possible.[242] As a result of the cost of $GeO_2$, work involving full cell systems has focused on the silicates. So far, power outputs have been relatively low, e.g. Yoshioka et al. have reported a maximum output of 120 mW cm$^{-2}$ at 800 °C for a fuel cell with a Mg doped $La_{9.8}(SiO_4)_{5.7}(MgO_4)_{0.3}O_{2.4}$ electrolyte, a lanthanum cobaltate cathode and a Ni/Ceria anode.[238] This, however, represented a significant improvement over earlier work with the use of Pt electrodes, suggesting that

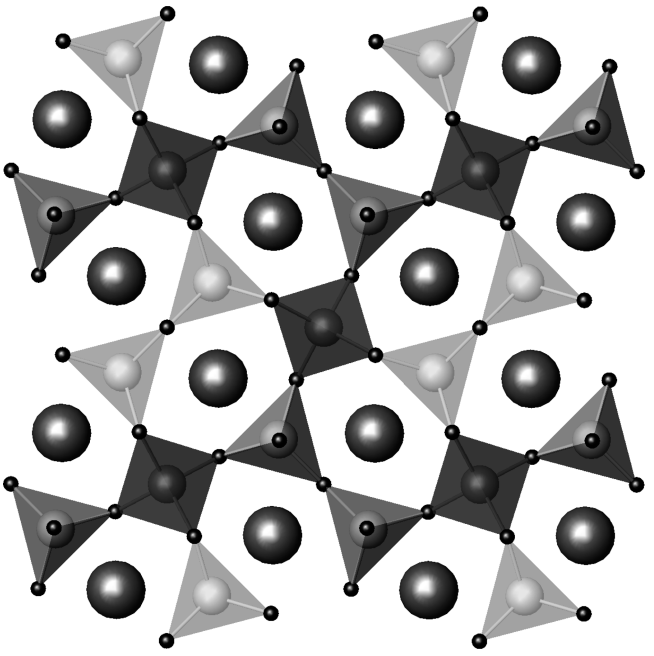

**Figure 6.** Melilite structure adopted by $LaSrGa_3O_7$ (tetrahedra = $GaO_4$ units (dark = Ga1 site, light = Ga2 site), large dark spheres = La/Sr). The Ga2 sites are believed to raise their coordination sphere to allow the incorporation of additional interstitial oxide ions.

further improvements can be made through electrode optimization and, hence, identifying the need for more work in optimizing electrodes for use with apatite electrolytes. In this respect, there have been comparatively few studies of the compatibility of these apatite systems with fuel cell electrodes.[243−245] McFarlane et al. examined the reactivity of a range of fuel cell cathodes with $La_{9.33}(SiO_4)_6O_2$ at 1350 °C, which showed no secondary phases, but some interdiffusion of the transition metals (Fe, Co, Mn) into the apatite phase.[243] Kharton and co-workers have also tested different cathodes on apatite $La_{10}(SiO_4)_5(AlO_4)O_{2.5}$ electrolytes. They examined a range of perovskite manganates and Ruddlesen−Popper nickelates finding that the Ni based cathodes showed better performance, with the manganates ($SrMn_{0.6}Nb_{0.4}O_{3-\delta}$, $Sr_{0.7}Ce_{0.3}Mn_{0.9}Cr_{0.1}O_{3-\delta}$, and $Gd_{0.6}Ca_{0.4}Mn_{0.9}Ni_{0.1}O_{3-\delta}$) showing significant cation interdiffusion between electrode and electrolyte.[245] In addition, there are some concerns regarding the potential poisoning of the electrode materials due to the presence of Si in these systems, with reported problems with surface diffusion of silica from a $La_{10}(SiO_4)_5(AlO_4)O_{2.5}$ electrolyte leading to a blocking of the electrode−electrolyte interface

The potential use of these apatite systems in SOFCs with $NH_3$ as a fuel has also been studied, with the results suggesting problems with this fuel at elevated temperatures (≥800 °C) due to significant nitridation: the O/N exchange process ($2N^{3-}$ replacing $3O^{2-}$) reducing the interstitial oxide ion content.[246] Silica volatility has also been reported on extended heat treatment at elevated temperatures (>800 °C) in $NH_3$ and $H_2$, suggesting that fuel cell operation be limited to below this temperature.[245,246] Overall, these apatite systems show substantial promise, although there is a need for further compatibility studies on alternative compositions, for example the Mg doped silicates, as well as further full cell tests to determine their true potential.

**3.3. Other Oxide Ion Conductors.** Another material in which the accommodation of interstitial oxide ions has been shown to be possible is the layered tetrahedral network melilite structure (Figure 6). Rosseinsky and co-workers have reported high oxide ion conductivity ($\sigma$ = 0.02−0.1 S cm$^{-1}$ between 600 and 900 °C for $La_{1+x}Sr_{1-x}Ga_3O_{7+x/2}$ ($x$ = 0.54)) in such systems.[247] The interstitial oxide ions are accommodated by the ability of Ga to raise its coordination network, and the flexibility of the structure allowing local relaxation around the interstitial oxide ion defect. Indeed, this observation as well as the work on apatite systems suggest that further doping studies to introduce interstitial oxide ions should be tried for other structure-types in the search for additional interstitial oxide ion conductors (traditionally doping studies have focused solely on the potential introduction of oxide ion vacancies).

In terms of other gallate systems, the cuspidine-type materials, $Ln_4(Ga_2O_7)O_2$ (Ln = rare earth), have also shown respectable conductivities. The structures of these systems consist of chains of edge-sharing $LnO_7/LnO_8$ polyhedra interconnected through the $Ga_2O_7$ units. By suitable doping with a higher valent cation, e.g. $Ln_4(Ga_{2-x}M_xO_{7+x/2})O_2$ (M = Ti, Ge),[248−251] it is possible to incorporate extra oxygen, which converts the isolated $M_2O_7$ groups into chains of distorted trigonal bipyramids, as observed for $La_4(Ti_2O_8)O_2$. The highest conductivities ($\approx 1 \times 10^{-3}$ S cm$^{-1}$ at 800 °C) were reported for $Nd_4(Ga_{1.2}Ge_{0.8}O_{7.4})O_2$. For the Ti doped samples, lower conductivities are observed, although these systems also show evidence for proton conductivity below 700 °C in wet atmospheres. An interesting feature of these materials is their conduction mechanism, which for oxide ion migration has been predicted by computer modeling studies to proceed via a cooperative vacancy migration process involving significant rotational motion.[252] Despite the interesting features of these cuspidine systems, their conductivities are rather too low for SOFC electrolyte applications, although the modeling studies have predicted that a low energy interstitial migration mechanism may be possible for the fully Ti doped endmember, $La_4(Ti_2O_8)O_2$, if suitable doping to introduce oxide ion excess could be achieved.

**3.4. New Proton Conductors.** Materials that show high oxide ion conductivity can also display proton conduction in wet atmospheres, as highlighted above for the Ti doped cuspidine systems. This occurs due to water incorporation into the vacant oxide ion sites (eq 1). The perovskite systems, $BaZr_{1-x}M_xO_{3-x/2}$ and $BaCe_{1-x}M_xO_{3-x/2}$ (M = trivalent cation) continue to dominate the research on proton conductors, as outlined in the Introduction.

In terms of newer chemical systems, there appears to be a growing trend toward structure types containing tetrahedral moieities. Thus, initially there was significant interest in lanthanide phosphate systems, with alkaline earth doped $LaPO_4$ showing respectable proton conductivity

($\approx 3 \times 10^{-4}$ S cm$^{-1}$ at 900 °C).[253,254] Subsequently higher conductivities were reported by Norby et al. for the alkaline earth doped $LaMO_4$ (M = Nb, Ta).[255] An unusual feature of both these systems is that the conductivity enhancement is observed for very low doping levels (≈1 at %). Indeed higher dopant levels have not so far been achieved in these systems. The conductivities of these $LaMO_4$ systems are lower than the perovskites ($\approx 10^{-3}$ S cm$^{-1}$ at 800 °C), but they show much higher stabilities in $CO_2$ containing atmospheres. For the phosphate systems, NMR has suggested that the oxide ion vacancies are accommodated by the formation of $P_2O_7^{4-}$ units, which when hydrated produce $HPO_4^{2-}$ units.[253] Similarly, recent modeling work on $LaNbO_4$ has suggested the formation of $Nb_3O_{11}^{7-}$ defect clusters to accommodate the oxide ion vacancies.[256]

In terms of moving toward electrolyte applications of these systems, methods for producing dense membranes have been examined, and the synthesis of fine particle size samples of $La_{1-x}A_xNbO_4$ ($x = 0$, 0.005, 0.02; A = Ca, Sr, Ba) via a spray pyrolysis route has been shown to be successful in producing dense (>97% theoretical) pellets at 1200 °C, lowered by a further 150 °C by hot pressing (25 MPa).[257] In addition, the chemical compatibility with fuel cell electrodes has been examined. This work has shown good compatibility with Ni anodes and perovskite cathodes, although reaction was observed with $La_2NiO_{4+\delta}$ cathodes.[258]

Similar proton conductivities have also been observed in the gallate systems, $La_{1-x}Ba_{1+x}GaO_{4-x/2}$ and $La_{1-x}(Sr/Ba)_{2+x}GaO_{5-x/2}$ ($0 \le x \le 0.2$), containing tetrahedral $GaO_4$, although the latter systems suffer from stability problems.[259] The $La_{1-x}Ba_{1+x}GaO_{4-x/2}$ system has therefore been examined further and small improvements in the proton conductivity were achieved by partial substitution of Pr for La ($\sigma \approx 3 \times 10^{-4}$ S cm$^{-1}$ at 500 °C for $La_{0.7}Pr_{0.2}Ba_{1.1}GaO_{3.95}$[260]). In this system, oxide ion vacancies are accommodated by the formation of $Ga_2O_7$ units, which are then broken up on water incorporation.[261] The related Al containing analogue has also been examined, although slightly lower conductivities were observed.[260]

Overall in the proton conductor area, the perovskite systems continue to dominate, but the $CO_2$ stability of the $LaMO_4$ systems gives them promise.

## 4. Anode Materials

As noted in the Introduction, the most widely utilized anode material is a Ni/electrolyte cermet, although there is growing interest in cermets with Cu. These anodes offer excellent performance particularly with $H_2$ as the fuel. However, they are not without their problems. In particular, with hydrocarbon fuels, catalytic cracking by Ni can lead to carbon build up and hence poisoning of the anode, especially if the steam concentration in the fuel stream is low. In addition, the presence of S within the fuel, present in significant levels in natural gas, will also lead to poisoning through the formation of $NiS_x$. There has therefore been a lot of interest in the development of anodes that are not susceptible to coking or sulfur poisoning. Consequently, there is a great deal of interest in alternative anodes, and in this respect, there has been a large focus on mixed metal oxide anode systems.

The research on mixed metal oxide anodes has been driven by the belief that they will be less susceptible to coking or S poisoning. In terms of such mixed metal oxide systems, the need for high electronic conductivity in the anode has focused attention particularly on perovskite materials. A key concern with respect to the utilization of mixed metal oxide anodes is the reducibility of the anode, leading potentially to complete reduction to the metal and hence decomposition. Hence, such anodes should contain transition metals that are stable against such complete reduction under solid oxide fuel cell operating conditions. As a result, early work in this area focused on titanate and titanate−niobate systems, due to the intrinsic stability of such materials at high temperatures in reducing conditions. $SrTiO_3$ itself is relatively difficult to reduce, and hence, low conductivities are observed even at high temperatures in reducing conditions. However, through suitable doping, enhancements in the conductivity can be achieved. For these titanates, a rich wealth of defect chemistry is accessible, with samples containing cation vacancies, anion vacancies, and anion excess being investigated.

Initial work focused on doping with either Nb (for Ti) or La (for Sr), with charge balance by the introduction of cation vacancies, i.e. $Sr_{1-x/2}Ti_{1-x}Nb_xO_3$ and $Sr_{1-3x/2}La_xTiO_3$.[262,263] These cation deficient samples showed respectable conductivities (≈10 S cm$^{-1}$) at elevated temperatures under reducing conditions and were stable under both oxidizing and reducing conditions. Hence, they could be prepared in air and then reduced in the anode environment. This is an important feature, as it means that it is easily possible to regenerate the properties of the anode if there is a leak in the fuel cell. However, despite these good properties, they suffer from poor oxide ion conductivity, which can be attributed to the low levels of oxide ion vacancies. Consequently, other systems were investigated, and it was shown that by doping with Nb to higher levels, related tungsten bronze phases, $(Sr/Ba)_{0.6}Ti_{0.2}Nb_{0.8}O_3$, could be prepared, which appeared to show more promising behavior than the corresponding perovskites.[264] However, these still suffered from poor oxide ion conductivity, and similar problems were observed for other tungsten bronze phases, $(Ba, Sr, Ca, La)_{0.6}M_xNb_{1-x}O_3$ (M = Ni, Mg, Mn, Fe, Cr, In, Sn).[265] Further doping studies in both perovskite and tungsten bronze systems to improve the ionic conductivity by introducing oxide ion vacancies have been unsuccessful.[266,267]

Subsequently oxygen rich perovskites, $Sr_{1-x}La_xTiO_{3+\delta}$, have attracted significant attention. These materials consist of perovskite slabs separated by crystallographic shears, which allow the accommodation of the excess oxygen. They may be classed as an homologous series, with the general formula $La_4Sr_{n-4}Ti_nO_{3n+2}$, with most of the research focusing on the $n = 12$ member of this series.

The presence of excess oxygen makes these materials readily reducible, and conductivities as high as 60 S $cm^{-1}$ have been reported at elevated temperatures under reducing conditions.[268] Despite some promise, this system also suffers from relatively poor oxide ion kinetics, and hence, doping studies have been attempted to improve this characteristic. In particular, the partial substitution of Ti by Mn/Ga/Sc has been examined, since these dopants are capable of accommodating lower coordination numbers, and so potentially enhancing oxide ion conductivity.[269−273] These doping strategies tended to reduce the electronic conductivity slightly but were shown to enhance the fuel cell anode performance, expecially with $CH_4$ fuel. Particularly promising performance was observed for the $La_4Sr_8Ti_{11}Mn_{0.5}Ga_{0.5}O_{38-\delta}$/YSZ composite anode. With this anode, polarization resistances (e.g., 0.12 Ω $cm^2$ in wet $H_2$ at 950 °C) which were 15 times lower than the undoped system were obtained.[271] However, there is still the need to improve the electronic conduction of these titanate anodes further, as their lateral conductivity is rather low when employed as a composite anode with the electrolyte.

Higher electronic conductivities have been observed in titanate perovskites by prereducing at higher temperatures. Thus, for example, the conductivity of $Sr_{0.86}Y_{0.08}TiO_{3-\delta}$ prereduced at 1400 °C has been reported to be increased to 82 S $cm^{-1}$ at 800 °C.[274] Similarly, even higher conductivities have been reported by Karczewski et al. by prereducing in $NH_3$ rather than $H_2$, with the enhancement attributed to N incorporation.[275] A conductivity of 600 S $cm^{-1}$ was observed for $Sr_{0.92}Y_{0.08}Ti_{0.92}Nb_{0.08}O_{3-\delta}$ prereduced at 1500 °C in $NH_3$. However, such high temperature in situ reduction is not practical for anode supported SOFC applications, since it would lead to reactivity between cell components and densification of electrode layers. Hence, such an approach could only be employed for electrolyte supported systems.

Another way to raise the electronic conductivity is the introduction of other transition metals, e.g. Cr and Mn, showing variable oxidation states, but with sufficient stability under reducing conditions. $La_{1-x}A_xCrO_3$ materials have been typically investigated for applications as SOFC interconnect materials due to their reasonable electronic conductivity and stability at elevated temperatures under both oxidizing and reducing conditions. As a consequence of these properties, the potential of these systems as anode materials has also been investigated, although the performance of the pure perovskite chromates was shown to be rather poor. Through partial substitution of Cr by other transition metal ions, e.g. Mn, Fe, V, Ni, improvements in performance were observed.[276−280]

In this respect, an important initial advance was the report by Irvine and Tao of promising anode performance for the mixed Cr/Mn system, $(La/Sr)_{1-x}Cr_{0.5}Mn_{0.5}O_{3-\delta}$ ($0 \le x \le 0.1$).[278,281] This material is stable at elevated temperature in both oxidizing and reducing conditions, with the conductivity shown to be essentially p-type, being higher in oxidizing conditions ($\sigma = 20-35$ S $cm^{-1}$ in oxidizing conditions, and 1−3 S $cm^{-1}$ in reducing conditions). This anode material was shown to give stable operation in methane with low steam concentrations in the fuel stream. Oxide ion diffusion coefficients determined through SIMS techniques gave values of $3 \times 10^{-8}$ and $4 \times 10^{-10}$ $cm^2$ $s^{-1}$ at 1000 °C in reducing and oxidizing conditions respectively.[282] Thus, whereas the electronic conductivity decreases slightly with decreasing $p(O_2)$, there is a significant increase in the oxide ion conductivity due to the introduction of oxide ion vacancies. The increasing ionic conductivity in reducing conditions has also been confirmed by detailed studies by Kharton et al.[283] However, as with the perovskite titanate systems, the oxide ion conductivity is still relatively low. In addition, the catalytic activity is also relatively low. In order to improve the performance of these anodes, composite systems containing the electrolyte and a metal (Ni, Cu) have been prepared. Liu et al. have shown that the addition of a small amount of Ni (4%) to a $(La/Sr)_{1-x}(Cr/Mn)O_{3-\delta}$/CGO composite leads to a significantly improved performance with hydrocarbon fuels.[284] The Ni introduces additional catalytic performance, while the low levels used appear to avoid problems of C formation. Other additives to improve catalytic performance have included $CeO_2$ and Pd, with both reported to improve performance with $CH_4$ fuel, without the observation of C deposition.[285,286] In addition, recently improved performance in $CH_4$ has been reported for the Ce doped system, $La_{0.65}Ce_{0.1}Sr_{0.25}Cr_{0.5}Mn_{0.5}O_3$.[287] These Cr/Mn systems have also been shown to display improved stability in the presence of S compared to Ni/YSZ anodes, although Chen et al. did observe the presence of S containing impurities after stability testing for 120 h in wet 99.5% $CH_4$/0.5% $H_2S$.[286]

Dopants other than Mn have also been investigated for $La_{1-x}A_xCrO_3$ materials. Ni doping has been shown to improve anode performance. Thus, Sauvet et al. have reported $La_{1-x}Sr_xCr_{1-y}Ni_yO_{3-\delta}$ as potential anode systems, with the highest catalytic activity observed for the composition with $x = 0.3$ and $y = 0.05$.[277] Similarly, $Pr_{0.7}Sr_{0.3}Cr_{0.9}Ni_{0.1}O_{3-\delta}$ has been reported as a redox stable anode, with conductivities of 27 and 1.4 S $cm^{-1}$ at 900 °C in air and 5% $H_2$, respectively.[288] One question mark over these Ni doped systems has been, however, whether the improved performance is partly due to Ni precipitating from the material on reduction. Partial substitution of Cr by V and Ru has also been exploited to improve the catalytic activity.[276]

Vanadate perovskites, e.g. $Sr_{1-x}La_xVO_3$, have also attracted some attention, due to their very high electronic conductivities.[289,290] However, these phases are unstable in higher $p(O_2)$, while a further problem is the high volume change on reduction, which limits any tolerance to reoxidation. More promising potential has been observed for the Mo doped vanadate, $CaV_{0.5}Mo_{0.5}O_{3-\delta}$, which transforms to a scheelite-type structure on oxidation, with the thermal expansion coefficients of both the reduced and oxidized phases being similar both to each other and other SOFC components.[291] Very high electronic

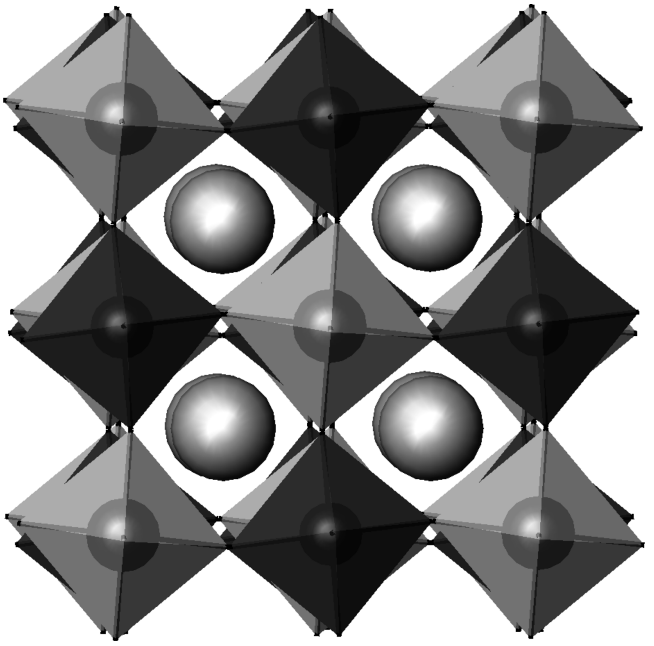

**Figure 7.** Double perovskite structure adopted by $Sr_2MgMoO_6$ (dark octahedra = $MoO_6$, light octahedra = $MgO_6$, large white spheres = Sr).

conductivities ($>525$ S cm$^{-1}$) were observed for the reduced phase.

Indeed, Mo containing perovskites have become promising candidates for S tolerant anodes, following important work in this area by Huang et al.[292−294] This group investigated the double perovskites $Sr_2Mg_{1-x}Mn_xMoO_{6-\delta}$ as potential anode materials (Figure 7). The phases were shown to be stable in both oxidizing and reducing conditions, with oxide ion vacancies introduced on reduction (typically $\delta \approx 0.05$),[295] which can be accommodated by the presence of B site cations with the ability to vary their coordination number. These systems therefore offer high electronic conductivity coupled with oxide ion conductivity. All the compositions showed good anode performance, although those higher in Mg content were shown to have the best performance. In addition, these systems showed good stability in both $H_2$ and $CH_4$ fuels, along with a good tolerance to S. One potential problem is Mo diffusion into the electrolyte, although this can be overcome by the use of a ceria-based buffer layer between anode and electrolyte. Further improvements in performance have been reported on La doping,[296] although such phases have also been reported to be unstable under oxidizing conditions.[297] In addition, similar good anode performances have been reported for $Sr_2CoMoO_6$, although there have been contradictory reports for $Sr_2NiMoO_6$.[294,298] Overall these molybdates show significant promise, with high power densities observed for fuel cells employing these as anodes, warranting further detailed studies.

In terms of nonperovskite related anodes, $TiO_2$ doped YSZ/ScSZ have been examined, although the relatively low ($<20\%$) Ti solubility in the lattice resulted in electronic conductivities that were far too low for suitable anode applications ($\approx$0.1 S cm$^{-1}$ at 900 °C).[299,300] Similarly there has been limited work on pyrochlore-type materials, $Ln_2Ti_2O_7$. However, as for the perovskite titanates, very high temperature prereduction is required to achieve the requisite high electronic conductivity.[301]

## 5. Conclusions

The need for improved energy efficiency has driven solid oxide fuel cells to the forefront of research into efficient electricity production. Traditionally, research into new materials has been rather narrowly focused, with an emphasis on fluorite and perovskite systems. Whereas these two structure-types continue to dominate the literature in this field, there is growing interest in alternative structure types. In this review, we have shown that such research into alternative systems is particularly prevalent in the electrolyte area. In this area, there has been an emergence of materials displaying high oxide ion conduction due to the presence of interstitial oxide ion defects. Such systems have also found promise in the electrode areas, where oxygen excess materials with the $K_2NiF_4$ structure have attracted considerable interest as cathodes, while oxygen excess perovskite titanates have shown promise as anodes. For all these areas, the identification of the "perfect" material remains fraught with difficulty, due to the wide range of requirements for SOFC materials, whether anode, cathode, or electrolyte. Consequently, materials selection requires substantial compromise between the individual requirements, and so, the true potential of these new materials will only become apparent with further detailed full cell testing and optimization.

## References


(1) Goodenough, J. B. *Annu. Rev. Mater. Res.* **2003**, *33*(1), 91.
(2) Kendall, K. R.; Navas, C.; Thomas, J. K.; zurLoye, H. C. *Solid State Ionics* **1995**, *82*(3−4), 215.
(3) Baur, E.; Preis, H. *Z. Elktrochem.* **1937**, *43*, 727.
(4) Badwal, S. P. S.; Ciacchi, F. T.; Milosevic, D. *Solid State Ionics* **2000**, *136*, 91.
(5) Kharton, V. V.; Marques, F. M. B.; Atkinson, A. *Solid State Ionics* **2004**, *174*, 135.
(6) Gorelov, V. P.; Palguev, S. F. *Doklady Akademii Nauk Sssr* **1979**, *248* (6), 1356–1359.
(7) Kharton, V. V.; Naumovich, E. N.; Vecher, A. A. *J Solid State Electrochem* **1999**, *3*, 61.
(8) Yamamoto, O.; Arachi, Y.; Sakai, H.; Takeda, Y.; Imanishi, N.; Mizutani, Y.; Kawai, M.; Nakamaru, Y. *Ionics* **1998**, *4*, 403.
(9) Tuller, H. L.; Nowick, A. S. *J. Electrochem. Soc.* **1975**, *122*(2), 255.
(10) Doshi, R.; Richards, V. L.; Carter, J. D.; Wang, X. P.; Krumpelt, M. *J. Electrochem. Soc.* **1999**, *146*(4), 1273.
(11) Inoue, T.; Setoguchi, T.; Eguchi, K.; Arai, H. *Solid State Ionics* **1989**, *35*(3−4), 285.
(12) Kudo, T.; Obayashi, H. *J. Electrochem. Soc.* **1976**, *123*(3), 415.
(13) Eguchi, K.; Setoguchi, T.; Inoue, T.; Arai, H. *Solid State Ionics* **1992**, *52*(1−3), 165.
(14) Mogensen, M.; Sammes, N. M.; Tompsett, G. A. *Solid State Ionics* **2000**, *129*(1−4), 63.
(15) Kharton, V. V.; Figueiredo, F. M.; Navarro, L.; Naumovich, E. N.; Kovalevsky, A. V.; Yaremchenko, A. A.; Viskup, A. P.; Carneiro, A.; Marques, F. M. B.; Frade, J. R. *J. Mater. Sci.* **2001**, *36*(5), 1105.
(16) Kosacki, I.; Suzuki, T.; Petrovsky, V.; Anderson, H. U. *Solid State Ionics* **2000**, *136*, 1225–1233.
(17) Kim, S.; Anselmi-Tambtirini, U.; Park, H. J.; Martin, M.; Munir, Z. A. *Adv. Mater.* **2008**, *20*(3), 556.
(18) Anselmi-Tamburini, U.; Maglia, F.; Chiodelli, G.; Riello, P.; Bucella, S.; Munir, Z. A. *Appl. Phys. Lett.* **2006**, *89*, 163116.
(19) Kosacki, I.; Rouleau, C. M.; Becher, P. F.; Bentley, J.; Lowndes, D. H. *Solid State Ionics* **2005**, *176*(13−14), 1319.
(20) Chiodelli, G.; Maglia, F.; Anselmi-Tamburini, U.; Munir, Z. A. *Solid State Ionics* **2009**, *180*(4−5), 297.

(21) Kim, S.; Avila-Paredes, H. J.; Wang, S. Z.; Chen, C. T.; Souza, De; Martin, R. A.; Munir, M. *Phys. Chem. Chem. Phys.* **2009**, *11*(17), 3035.
(22) Ruiz-Trejo, E.; Kilner, J. A. *J. Appl. Electrochem.* **2009**, *39*(4), 523.
(23) Takahashi, T.; Iwahara, H.; Arao, T. *J. Appl. Electrochem.* **1975**, *5*, 187.
(24) Hapase, M. G.; Tare, V. B.; Biswas, A. B. *Indian J. Pure Appl. Phys.* **1967**, *5*, 1.
(25) Fruth, V.; Ianculescu, A.; Berger, D.; Preda, S.; Voicu, G.; Tenea, E.; Popa, M. *J. Eur. Ceram. Soc.* **2006**, *26*(14), 3011.
(26) Verkerk, M. J.; van de Velde, G. M. H.; Burggraaf, A. J.; Helmholdt, R. B. *J. Phys. Chem. Solids* **1982**, *43*(12), 1129.
(27) Harwig, H. A.; Gerards, A. G. *Thermochim. Acta* **1979**, *28*(1), 121.
(28) Takahashi, T.; Iwahara, H. *Mater. Res. Bull.* **1978**, *13*(12), 1447.
(29) Iwahara, H.; Esaka, T.; Sato, T.; Takahashi, T. *J. Solid State Chem.* **1981**, *39*(2), 173.
(30) Miyayama, M.; Yanagida, H. *Mater. Res. Bull.* **1986**, *21*(10), 1215.
(31) Battle, P. D.; Hu, G.; Moroney, L. M.; Munro, D. C. *J. Solid State Chem.* **1987**, *69*(1), 30.
(32) Jaiswal, A.; Wachsman, E. D. *Solid State Ionics* **2006**, *177*(7−8), 677.
(33) Watanabe, A. *Solid State Ionics* **2005**, *176*(31−34), 2423.
(34) Watanabe, A.; Sekita, M. *Solid State Ionics* **2005**, *176*(31−34), 2429.
(35) Lee, Y. J.; Park, C. O.; Baek, H. D.; Hwang, J. S. *Solid State Ionics* **1995**, *76*(1−2), 1.
(36) Ling, C. D.; Withers, R. L.; Schmid, S.; Thompson, J. G. *J. Solid State Chem.* **1998**, *137*(1), 42.
(37) Jiang, N.; Wachsman, E. D.; Jung, S. *Solid State Ionics* **2002**, *150* (3−4), 347.
(38) Meng, G.; Chen, C.; Han, X.; Yang, P.; Peng, D. *Solid State Ionics* **1988**, *28*−*30*, 533.
(39) Yaremchenko, A. A.; Kharton, V. V.; Naumovich, E. N.; Tonoyan, A. A. *Mater. Res. Bull.* **2000**, *35*(4), 515.
(40) Azad, A. M.; Larose, S.; Akbar, S. A. *J. Mater. Sci.* **1994**, *29*(16), 4135.
(41) Shuk, P.; Wiemhofer, H. D.; Guth, U.; Gopel, W.; Greenblatt, M. *Solid State Ionics* **1996**, *89*(3−4), 179.
(42) Subramanian, M.; Aravamudan, G.; Subba Rao, G. V. *Prog. Solid State Chem.* **1983**, *15*, 55.
(43) Tuller, H. L. *Solid State Ionics* **1992**, *52*(1−3), 135.
(44) Tuller, H. L.; Moon, P. K. *Mater. Sci. Eng.: B* **1988**, *1*(2), 171.
(45) Wilde, P. J.; Catlow, C. R. A. *Solid State Ionics* **1998**, *1*(12), 173.
(46) Díaz-Guillén, J. A.; Fuentes, A. F.; Díaz-Guillén, M. R.; Almanza, J. M.; Santamaría, J.; León, C. *J. Power Sources* **2009**, *186*(2), 349.
(47) Shimura, T.; Komori, M.; Iwahara, H. *Solid State Ionics* **1996**, *86*−*88*, 685.
(48) Omata, T.; Okuda, K.; Tsugimoto, S.; Otsuka-Yao-Matsuo, S. *Solid State Ionics* **1997**, *104*, 249.
(49) Omata, T.; Otsuka-Yao-Matsuo, S. *J. Electrochem. Soc.* **2001**, *148*, E252.
(50) Björketun, M. E.; Knee, C. S.; Nyman, B. J.; Wahnström, G. *Solid State Ionics* **2008**, *178*(31−32), 1642.
(51) Eurenius, K. E. J.; Ahlberg, E.; Ahmed, I.; Eriksson, S. G.; Knee, C. S. *Solid State Ionics*, DOI: 10.1016/j.ssi.2009.05.004.
(52) Feng, M.; Goodenough, J. B. *Eur. J. Solid State Inorg. Chem.* **1994**, *31*, 663.
(53) Ishihara, T.; Matsuda, H.; Takita, Y. *J. Am. Chem. Soc.* **1994**, 116.
(54) Stevenson, J. W.; Hasinska, K.; Armstrong, T. R. *Solid Oxide Fuel Cells* (*Sofc VI*) **1999**, *99*(19), 275.
(55) Ishihara, T.; Shibayama, T.; Nishiguchi, H.; Takita, Y. *J. Mater. Sci.* **2001**, *36*, 1125.
(56) Ishihara, T.; Furutani, H.; Honda, M.; Yamada, T.; Shibayama, T.; Akbay, T.; Sakai, N.; Yokokawa, H.; Takita, Y. *Chem. Mater.* **1999**, *11*(8), 2081.
(57) Trofimenko, N.; Ullmann, H. *Solid State Ionics* **1999**, *118*(3−4), 215.
(58) Takahashi, T.; Iwahara, H. *Rev. Chim. Miner.* **1980**, *17*, 243.
(59) Kreuer, K. D. *Chem. Mater.* **1996**, *8*(3), 610.
(60) Iwahara, H.; Uchida, H.; Maeda, N. *J. Power Sources* **1982**, *7*, 293.
(61) Norby, T.; Kofstad, P. *Solid State Ionics* **1986**, *20*, 169.
(62) Münch, W.; Seifert, G.; Kreuer, K.-D.; Maier, J. *Solid State Ionics* **1996**, *86*−*88*, 647.
(63) Iwahara, H.; Esaka, T.; Uchida, H.; Maeda, N. *Solid State Ionics* **1981**, *3*−*4*, 359.
(64) Iwahara, H.; Uchida, H.; Ono, K.; Ogaki, K. *J. Electrochem. Soc.* **1988**, *135*(2), 529.
(65) Iwahara, H.; Yajima, T.; Hibino, T.; Ozaki, K.; Suzuki, H. *Solid State Ionics* **1993**, *61*, 65.
(66) Ryu, K. H.; Haile, S. M. *Solid State ionics* **1999**, *125*, 355.
(67) Babilo, P.; Haile, S. M. *J. Am. Ceram. Soc.* **2005**, *88*, 2362.
(68) Tao, S. W.; Irvine, J. T. S. *Adv. Mater.* **2006**, *18*, 1581.
(69) Nowick, A. S.; Du, Y.; Liang, K. C. *Solid State Ionics* **1999**, *125*, 303.
(70) Liang, K. C.; Du, Y.; Nowick, A. S. *Solid State Ionics* **1994**, *69*(2), 117.
(71) Du, Y.; Nowick, A. S. *J. Am. Ceram. Soc.* **1995**, *78*(11), 3033.
(72) Corcoran, D. J. D.; Irvine, J. T. S. *Solid State Ionics* **2001**, *145*, 307.
(73) Goodenough, J. B.; Ruizdiaz, J. E.; Zhen, Y. S. *Solid State Ionics* **1990**, *44*, 21.
(74) Berastegui, P.; Hull, S.; Garcia-Garcia, F. J.; Eriksson, S. G. *J. Solid State Chem.* **2002**, *164*(1), 119.
(75) Shimura, T.; Yogo, T. *Solid State Ionics* **2004**, *175*(1−4), 345.
(76) Jayaraman, V.; Magrez, A.; Caldes, M.; Joubert, O.; Ganne, M.; Piffard, Y.; Brohan, L. *Solid State Ionics* **2004**, *170*, 17.
(77) Yao, T.; Uchimoto, Y.; Kinuhata, M.; Inagaki, T.; Yoshida, H. *Solid State Ionics* **2000**, *132*(3−4), 189.
(78) Schwartz, M.; Link, B. F.; Sammells, A. F. *J. Electrochem. Soc.* **1993**, *140*(4), L62.
(79) Rolle, A.; Vannier, R. N.; Giridharan, N. V.; Abraham, F. *Solid State Ionics* **2003**, *176*, 2095.
(80) Kakinuma, K.; Yamamura, H.; Haneda, H.; Atake *J. Therm. Anal. Calorim.* **1999**, *57*, 737.
(81) Liu, Y.; Withers, R. L.; Fitz, J. D. *J. Solid State Chem.* **2003**, *170*(2), 247.
(82) Hashimoto, T.; Yoshinaga, M.; Ueda, Y.; Komazaki, K.; Asaoka, K.; Wang, S. *J. Therm. Anal. Calorim.* **2002**, *69*, 909.
(83) Zhang, G. B.; Smyth, D. M. *Solid State Ionics* **1995**, *82*(3−4), 161.
(84) Goodenough, J. B.; Manthiram, A.; Kuo, J. F. *Mater. Chem. Phys.* **1993**, *35*, 221.
(85) Fisher, C. A. J.; Islam, M. S. *Solid State Ionics* **1999**, *118*, 355.
(86) Setoguchi, T.; Okamoto, K.; Eguchi, K.; Arai, H. *J. Electrochem. Soc.* **1992**, *139*, 2875.
(87) Spacil, H. S. Electrical device including Nickel-containing stabilised zirconia electrode. US Patent, 3503809, **1970**.
(88) Steele, B.; Heinzel, A. *Nature* **2001**, *414*, 345.
(89) Gorte, R.; Park, S.; Vohs, J.; Want, C. *Adv. Mater.* **2000**, *12*, 1465.
(90) Rostrup-Nielsen, J. R.; Sehested, J.; Nørskov, J. K. *Adv. Catal.* **2002**, *47*, 65.
(91) Mogensen, M.; Kammer, K. *Annu. Rev. Mater. Res.* **2003**, *33*, 321.
(92) Jiang, S. P.; Chan, S. H. *J. Mater. Sci.* **2004**, *39*, 4405.
(93) Wincewicz, K. C.; Cooper, J. S. *J. Power Sources* **2005**, *140*, 280.
(94) Cracium, R.; Park, S.; Gorte, R. J.; Vohs, J. M.; Wang, C.; Worrell, W. L. *J. Electrochem. Soc.* **1999**, *146*, 4019.
(95) Kiratzis, N.; Holtappels, P.; Hartwell, C. E.; Mogensen, M.; Irvine, J. T. S. *Fuel Cells* **2001**, *1*, 211.
(96) Ruiz-Morales, J. C.; Canales-Vazquez, J.; Marrero-Lopez, D.; Pena-Martinez, J.; Tarancon, A.; Irvine, J. T. S.; Nunez, P. *J. Mater. Chem.* **2008**, *18*, 5072.
(97) Klemenso, T.; Chung, C.; Larsen, P. H.; Mogensen, M. *J. Electrochem. Soc.* **2005**, *152*(11), A2186.
(98) Yamamoto, O.; Takeda, Y.; Kanno, R.; Noda, M. *Solid State Ionics* **1987**, *22*(2−3), 241.
(99) Skinner, S. J. *Int. J. Inorg. Mater.* **2001**, *3*(2), 113.
(100) Kuo, J. H.; Anderson, H. U.; Sparlin, D. M. *J. Solid State Chem.* **1989**, *83*, 52.
(101) Singhal, S. C. *Solid State Ionics* **2000**, *135*(1−4), 305.
(102) Teraoka, Y.; Nobunaga, T.; Okamoto, K.; Miura, N.; Yamazoe, N. *Solid State Ionics* **1991**, *48*, 207.
(103) Godickemeier, M.; Sasaki, K.; Gauckler, L. J.; Reiss, I. *Solid State Ionics* **1996**, *86*−*88*, 691.
(104) Kawada, T.; Masuda, K.; Suzuki, J.; Kaimai, A.; Kawamura, K.; Nigara, Y.; Mizusaki, J.; Yugami, H.; Arashi, H.; Sakai, N.; Yokokawa, H. *Solid State Ionics* **1999**, *121*, 271.
(105) Zhao, F.; Peng, R.; Xia, C. *Mater. Res. Bull.* **2008**, *43*(2), 370.
(106) Takeda, Y.; Ueno, H.; Imanishi, N.; Yamamoto, O.; Sammes, N.; Phillipps, M. B. *Solid State Ionics* **1996**, *86*−*88*, 1187.
(107) Hibino, T.; Hashimoto, A.; Inoue, T.; Tokuno, J.-I.; Yoshida, S.-I.; Sano, M. *Science* **2000**, *288*, 2031.
(108) Waller, D.; Lane, J. A.; Kilner, J. A.; Steele, B. C. H. *Mater. Lett.* **1995**, *27*, 225.
(109) Tai, L.-W.; Nasrallah, M. N.; Anderson, H. U.; Sparlin, D. M.; Sehlin, S. R. *Solid State Ionics* **1995**, *76*, 273.
(110) Skinner, S. J.; Kilner, J. A. *Solid State Ionics* **2000**, *135*, 709. Also: Skinner, S. J.; Kilner, J. A. *Ionics* **1999**, *5*, 3.
(111) Vashook, V. V.; Tolochko, S. P.; Yushkevich, I. I.; Makhnach, L. V.; Kononyuk, I. F.; Altenburg, H.; Hauck, J.; Ullmann, H. *Solid State Ionics* **1998**, *110*(3−4), 245.
(112) Kharton, V. V.; Viskup, A. P.; Naumovich, E. N.; Marques, F. M. B. *J. Mater. Chem.* **1999**, *9*, 2623.
(113) Amow, G.; Skinner, S. J. *J. Solid State Electrochem.* **2006**, *10*(8), 538.
(114) Boehm, E.; Bassat, J. M.; Steil, M. C.; Dordor, P.; Mauvy, F.; Grenier, J. C. *Solid State Sci.* **2003**, *5*(7), 973.
(115) Skinner, S. J.; Munnings, C. N.; Amow, G.; Whitfield, P.; Davidson, I. *Solid Oxide Fuel Cells VIII* (Electrochemical Society Series); **2003**, 7, 552.
(116) Sayers, R.; Liu, J.; Rustumji, B.; Skinner, S. J. *Fuel Cells* **2008**, *8*(5), 338.
(117) Solak, N.; Zinkevich, M.; Aldinger, F. *Solid State Ionics* **2006**, *177* (19−25), 2139.
(118) Zhao, H.; Mauvy, F.; Lalanne, C.; Bassat, J. M.; Fourcade, S.; Grenier, J. C. *Solid State Ionics* **2008**, *179*(35−36), 2000.
(119) Burriel, M.; Santiso, J.; Rossell, M. D.; Van Tendeloo, G.; Figueras, A.; Garcia, G. *J. Phys. Chem. C* **2008**, *112*(29), 10982.
(120) Briois, P.; Perry, F.; Billard, A. *Thin Solid Films* **2008**, *516*(10), 3282.
(121) Shaula, A. L.; Naumovich, E. N.; Viskup, A. P.; Pankov, V. V.; Kovalevsky, A. V.; Kharton, V. V *Solid State Ionics* **2009**, *180*(11−13), 812.
(122) Skinner, S. J.; Amow, G. *J. Solid State Chem.* **2007**, *180*(7), 1977.
(123) Wang, Y. S.; Nie, H. W.; Wang, S. R.; Wen, T. L.; Guth, U.; Valshook, V. *Mater. Lett.* **2006**, *60*(9−10), 1174.

(124) Jin, C.; Liu, J.; Zhang, Y. H.; Sui, J.; Guo, W. M. *J. Power Sources* **2008**, *182*(2), 482.
(125) Aguadero, A.; Alonso, J. A.; Escudero, M. J.; Daza, L. *Solid State Ionics* **2008**, *179*(11−12), 393.
(126) Zhao, F.; Wang, X.; Wang, Z.; Peng, R.; Xia, C. *Solid State Ionics* **2008**, *179*(27−32), 1450.
(127) Huang, J.; Jiang, X.; Li, X.; Liu, A. *J. Electroceram.* **2009**, *23*, 1.
(128) Li, Z. A.; Haugsrud, R.; Smith, J. B.; Norby, T. *J. Electrochem. Soc.* **2009**, *156*(9), B1039.
(129) Smith, J. B.; Norby, T. *J. Electrochem. Soc.* **2006**, *153*(2), A233.
(130) Mauvy, F.; Lalanne, C.; Bassat, J. M.; Grenier, J. C.; Zhao, H.; Huo, L. H.; Stevens, P. *J. Electrochem. Soc.* **2006**, *153*(8), A1547.
(131) Miyoshi, S.; Furuno, T.; Sangoanruang, O.; Matsumoto, H.; Ishihara, T. *J. Electrochem. Soc.* **2007**, *154*(1), B57.
(132) Sun, L.-P.; Li, Q.; Zhao, H.; Huo, L.-H.; Grenie, J.-C. *J. Power Sources* **2008**, *183*(1), 43.
(133) Yashima, M.; Enoki, M.; Wakita, T.; Ali, R.; Matsushita, Y.; Izumi, F.; Ishihara, T. *J. Am. Chem. Soc.* **2008**, *130*(9), 2762.
(134) Burriel, M.; Garcia, G.; Santiso, J.; Kilner, J. A.; Chater, R. J.; Skinner, S. J. *J. Mater. Chem.* **2008**, *18*, 416.
(135) Cleave, A. R.; Kilner, J. A.; Skinner, S. J.; Murphy, S. T.; Grimes, R. W *Solid State Ionics* **2007**, *179*(27−32), 823.
(136) Aguadero, A.; Alonso, J. A.; Fernandez-Diaz, M. T.; Escudero, M. J.; Daza, L. *J. Power Sources* **2007**, *169*(1), 17.
(137) Carvalho, M. D.; Costa, F. M. A.; Pereira, I. D. S.; Wattiaux, A.; Bassat, J. M.; Grenier, J. C.; Pouchard, M *J. Mater. Chem.* **1997**, *7*(10), 2107.
(138) Burriel, M.; Garcia, G.; Rossell, M. D.; Figueras, A.; Van Tendeloo, G.; Santiso, J. *Chem. Mater.* **2007**, *19*(16), 4056.
(139) Bannikov, D. O.; Cherepanov, V. A. *J. Solid State Chem.* **2006**, *179*(8), 2721.
(140) Weng, X. L.; Boldrin, P.; Abrahams, I.; Skinner, S. J.; Kellici, S.; Darr, J. A. *J. Solid State Chem.* **2008**, *181*(5), 1123.
(141) Maignan, A.; Martin, C.; Pelloquin, D.; Nguyen, N.; Raveau, B. *J. Solid State Chem.* **1999**, *142*(2), 247.
(142) Anderson, P. S.; Kirk, C. A.; Knudsen, J.; Reaney, I. M.; West, A. R. *Solid State Sci.* **2005**, *7*(10), 1149.
(143) Gu, H. T.; Chen, H.; Gao, L.; Zheng, Y. F.; Zhu, X. F.; Guo, L. C. *Int. J. Hydrogen Energy* **2009**, *34*(5), 2416.
(144) Taskin, A. A.; Lavrov, A. N.; Ando, Y. *Phys. Rev. B* **2005**, *71*(13), 28.
(145) Taskin, A. A.; Lavrov, A. N.; Ando, Y. *Appl. Phys. Lett.* **2005**, *86*(9), 3.
(146) Taskin, A. A.; Lavrov, A. N.; Ando, Y. *Prog. Solid State Chem.* **2007**, *35*(2−4), 481.
(147) Zhang, K.; Ge, L.; Ran, R.; Shao, Z.; Liu, S. *Acta Materialia* **2008**, *56* (17), 4876.
(148) (a) Kim, G.; Wang, S.; Jacobson, A. J.; Yuan, Z.; Donner, W.; Chen, C. L.; Reimus, L.; Brodersen, P.; Mims, C. A. *Appl. Phys. Lett.* **2006**, *88*, 024103-1. (b) Kim, G.; Wang, S.; Jacobson, A. J.; Reimus, L.; Brodersen, P.; Mims, C. A. *J. Mater. Chem.* **2007**, *17*(24), 2500.
(149) Chen, D. J.; Ran, R.; Zhang, K.; Wang, J.; Shao, Z. P. *J. Power Sources* **2009**, *188*(1), 96.
(150) Yang, C. L.; Wu, X. S.; Fang, S. M.; Chen, C. S.; Liu, W. *Mater. Lett.* **2009**, *63*(12), 1007.
(151) (a) Tarancón, A.; Pena-Martinez, J.; Marrero-Lopez, D.; Morata, A.; Ruiz-Morales, J. C.; Nuñez, P. *Solid State Ionics* **2008**, *179*(40), 2372. (b) Tarancon, A.; Skinner, S. J.; Chater, R. J.; Hernandez-Ramirez, F.; Kilner, J. A. *J. Mater. Chem.* **2007**, *17*(30), 3175.
(152) Chang, A. M.; Skinner, S. J.; Kilner, J. A. *Solid State Ionics* **2006**, *177* (19−25), 2009.
(153) Peña-Martínez, J.; Tarancón, A.; Marrero-López, D.; Ruiz-Morales, J. C.; Núñez, P. *Fuel Cells* **2008**, *8*(5), 351.
(154) Chen, D. J.; Ran, R.; Zhang, K.; Wang, J.; Shao, Z. P. *J. Power Sources* **2009**, *188*(1), 96–105.
(155) Zhou, Q. J.; He, T. M.; Ji, Y. *J. Power Sources* **2008**, *185*(2), 754.
(156) Sun, W. P.; Bi, L.; Yan, L. T.; Peng, R. R.; Liu, W. *J. Alloys Compd.* **2009**, *481*(1−2), L40.
(157) Zhou, Q.; He, T.; He, Q.; Ji, Y. *Electrochem. Commun.* **2009**, *11*(1), 80.
(158) Shao, Z. P.; Haile, S. M. *Nature* **2004**, *431*, 170.
(159) Shao, Z. P.; Haile, S. M.; Ahn, J.; Ronney, P. D.; Zhan, Z. L.; Barnett, S. A. *Nature* **2005**, *435*, 795.
(160) Zhou, W.; Ran, R.; Shao, Z. *J. Power Sources* **2009**, *192*(2), 231.
(161) Baumann, F. S.; Fleig, J.; Habermeier, H. U.; Maier, J. *Solid State Ionics* **2006**, *177*(35−36), 3187.
(162) Wang, L.; Merkle, R.; Maier, J.; Acarturk, T.; Starke, U. *Appl. Phys. Lett.* **2009**, 94.
(163) Li, S. Y.; Lu, Z.; Ai, N.; Chen, K. F.; Su, W. H. *J. Power Sources* **2007**, *165*, 97.
(164) Li, S. Y.; Lu, Z.; Huang, X. Q.; Su, W. H. *Solid State Ionics* **2008**, *178*, 1853.
(165) Li, S. Y.; Lu, Z.; Huang, X. Q.; Wei, B.; Su, W. H. *J. Phys. Chem. Solids* **2007**, *68*, 1707.
(166) Liu, Q. L.; Khor, K. A.; Chan, S. H. *J. Power Sources* **2006**, *161*, 123.
(167) Yan, A.; Cheng, M.; Dong, Y. L.; Yang, W. S.; Maragou, V.; Song, S. Q.; Tsiakaras, P. *Appl. Catal., B* **2006**, *66*(1−2), 64.
(168) Arnold, M.; Wang, H. H.; Feldhoff, A. *J. Membr. Sci.* **2007**, *293*(1−2), 44.
(169) Svarcova, S.; Wiik, K.; Tolchard, J.; Bouwmeester, H. J. M.; Grande, T. *Solid State Ionics* **2008**, *178*, 1787.
(170) Arnold, M.; Gesing, T. M.; Martynczuk, J.; Feldhoff, A. *Chem. Mater.* **2008**, *20*(18), 5851.
(171) Chiba, R.; Yoshimura, F.; Sakurai, Y. *Solid State Ionics* **1999**, *124* (3−4), 281.
(172) Komatsu, T.; Arai, H.; Chiba, R.; Nozawa, K.; Arakawa, M.; Sato, K *Electrochem. Solid State Lett.* **2006**, *9*(1), A9–A12.
(173) Millar, L.; Taherparvar, H.; Filkin, N.; Slater, P.; Yeomans, J. *Solid State Ionics* **2008**, *179*(19−20), 732.
(174) Swierczek, K.; Marzec, J.; Palubiak, D.; Zajac, W.; Molenda, J. *Solid State Ionics* **2006**, *177*(19−25), 1811–1817.
(175) Li, S.; Zhu, B. *J. Nanosci. Nanotechnol.* **2009**, *9*(6), 3824.
(176) Ehora, G.; Daviero-Minaud, S.; Steil, M. C.; Gengembre, L.; Frere, M.; Bellayer, S.; Mentré, O. *Chem. Mater.* **2008**, *20*(24), 7425.
(177) Camaratta, M.; Wachsman, E. *J. Electrochem. Soc.* **2008**, *155*(2), B135.
(178) Thompson, J. G.; Withers, R. L.; Brink, F. J. *J. Solid State Chem.* **1999**, *143*, 122.
(179) Skinner, S. J.; Kang, Y. *Solid State Sci.* **2003**, *5*, 1475.
(180) Tsipis, E. V.; Munnings, C. N.; Kharton, V. V.; Skinner, S. J.; Frade, J. R. *Solid State Ionics* **2006**, *177*, 1015.
(181) Packer, R. J.; Skinner, S. J.; Yaremchenko, A. A.; Tsipis, E. V.; Kharton, V. V.; Patrakeev, M. V.; Bakhteeva, Y. A. *J. Mater. Chem.* **2006**, *16*, 3503.
(182) Vullum, F.; Grande, T. *Solid State Ionics* **2007**, *179*, 1061.
(183) Zhang, Q.; Martin, B. E.; Petric, A. *J. Mater. Chem.* **2008**, *18*(36), 4341.
(184) Lacorre, P.; Goutenoire, F.; Bohnke, O.; Retoux, R.; Laligant, Y. *Nature* **2000**, *404*, 856.
(185) Evans, I. R.; Howard, J. A. K.; Evans, J. S. O. *Chem. Mater.* **2005**, *17*, 4074.
(186) Malavasi, L.; Kim, H.; Billinge, S. J. L.; Proffen, T.; Tealdi, C.; Flor, G. *J. Am. Chem. Soc.* **2007**, *129*, 6903.
(187) Hou, C. J.; Li, Y. D.; Wang, P. J.; Liu, C. S.; Wang, X. P.; Fang, Q. F.; Sun, D. Y. *Phys. Rev. B* **2007**, *76*, 014104.
(188) Marrero-Lopez, D.; Pena-Martinez, J.; Perez-Coll, D.; Nunez, P. *J. Alloy Comp* **2006**, *422*, 249.
(189) Marrero-Lopez, D.; Canales-Vazquez, J.; Zhou, W. Z.; Irving, J. T. S.; Nunez, P. *J. Solid State Chem.* **2006**, *179*, 278.
(190) Georges, S.; Bohnke, O.; Goutenoire, F.; Laligant, Y.; Fouletier, J.; Lacorre, P. *Solid State Ionics* **2006**, *177*, 1715.
(191) Basu, S.; Devi, P. S.; Maiti, H. S. *J. Electrochem. Soc.* **2005**, *152*, A2143.
(192) Tsai, D. S.; Hseih, M. J.; Tseng, J. C.; Lee, H. Y. *J. Eur. Ceram. Soc.* **2005**, *25*, 481.
(193) Georges, S.; Goutenoire, F.; Lacorre, P.; Steil, M. C. *J. Eur. Ceram. Soc.* **2005**, *25*, 3619.
(194) Wang, X. P.; Cheng, Z. J.; Fang, Q. F. *Solid State Ionics* **2005**, *176*, 761.
(195) He, T. M.; Huang, Y. L.; He, Q.; Jei, Y.; Pei, L.; Lui, J.; Lu, Z. *J. Alloy Comp.* **2005**, *388*, 145.
(196) Tealdi, C.; Chiodelli, G.; Malavasi, L.; Flor, G. *J. Mater. Chem.* **2004**, *14*, 3553.
(197) Georges, S.; Goutenoire, F.; Altorfer, F.; Sheptyakov, D.; Fauth, F.; Suard, E.; Lacorre, P. *Solid State Ionics* **2003**, *161*, 231.
(198) Arulraj, A.; Goutenoire, F.; Tabellout, M.; Bohnke, O.; Lacorre, P. *Chem. Mater.* **2002**, *14*, 2492.
(199) Georges, S.; Skinner, S. J.; Lacorre, P.; Steil, M. C. *Dalton Trans.* **2004**, 3101.
(200) Marrero-Lopez, D.; Ruiz-Morales, J. C.; Núñez, P.; Abrantes, J. C. C.; Frade, J. R. *J. Solid State Chem.* **2004**, *177*, 2378.
(201) Georges, S.; Rocha, R. A.; Djurado, E. *J. Phys. Chem. C* **2008**, *112*, 3194.
(202) Marrero-Lopez, D.; Pena-Martinez, J.; Ruis-Morales, J. C.; Perez-Coll, D.; Martin-Sedeno, M. C.; Nunez, P. *Solid State Ionics* **2007**, *178*, 1366.
(203) Corbel, G.; Lacorre, P. *J. Solid State Chem.* **2006**, *179*, 1339.
(204) Chang, H. C.; Tsai, D. S.; Chung, W. H.; Huang, Y. S.; Le, M. V. *Solid State Ionics* **2009**, *180*, 412.
(205) Zhuang, Z.; Wang, X. P.; Li, D.; Zhang, T.; Fang, Q. F. *J. Am. Ceram. Soc.* **2009**, *92*, 839.
(206) Nakayama, S.; Aono, H.; Sadaoka, Y. *Chem. Lett.* **1995**, 431.
(207) Nakayama, S.; Sakamoto, M.; Higuchi, M.; Kodaira, K. *J. Mater. Sci. Lett.* **2000**, *19*, 91.
(208) Arikawa, H.; Nishiguchi, H.; Ishihara, T.; Takita, Y. *Solid State Ionics* **2000**, *136−137*, 31.
(209) Pramana, S. S.; Klooster, W. T.; White, T. J. *Acta Cryst. B* **2007**, *63*, 597.
(210) Sansom, J. E. H.; Richings, D.; Slater, P. R. *Solid State Ionics* **2001**, *139*, 205.
(211) Leon-Reina, L.; Losilla, E. R.; Martinez-Lara, M.; Martin-Sedeno, M. C.; Bruque, S.; Nunez, P.; Sheptyakov, D. V.; Aranda, M. A. G. *Chem. Mater.* **2005**, *17*, 596.
(212) Kharton, V. V.; Shaula, A. L.; Patrakeev, M. V.; Waerenborgh, J. C.; Rojas, D. P.; Vyshatko, N. P.; Tsipis, E. V.; Yaremchenko, A. A.; Marques, F. M. B. *J. Electrochem. Soc.* **2004**, *151*, A1236.
(213) Sansom, J. E. H.; Tolchard, J. R.; Apperley, D.; Islam, M. S.; Slater, P. R. *J. Mater. Chem.* **2006**, *16*, 1410.

(214) Leon-Reina, L.; Porras-Vasquez, J. M.; Losilla, E. R.; Aranda, M. A. G. *J. Solid State Chem.* **2007**, *180*, 1250.
(215) Celerier, S.; Laberty-Robert, C.; Long, J. W.; Pettigrew, K. A.; Stroud, R. M.; Rolison, D. R.; Ansart, F.; Stevens, P. *Adv. Mater.* **2006**, *18*, 615.
(216) Chesnaud, A.; Bogicevic, C.; Karolak, F.; Estournes, C.; Dezaneau, G. *Chem. Commun.* **2007**, 1550.
(217) Orera, A.; Kendrick, E.; Apperley, D. C.; Orera, V. M.; Slater, P. R. *Dalton Trans.* **2008**, 5296.
(218) Pivak, Y. V.; Kharton, V. V.; Yaremchenko, A. A.; Yakovlev, S. O.; Kovalevsky, A. V.; Frade, J. R.; Marques, F. M. B. *J. Eur. Ceram. Soc.* **2007**, *27*, 2445.
(219) Kendrick, E.; Islam, M. S.; Slater, P. R. *J. Mater. Chem.* **2007**, *17*, 3104.
(220) Sansom, J. E. H.; Slater, P. R. *Solid State Ionics* **2004**, *167*, 23.
(221) Yoshioka, H. *J. Am. Ceram. Soc.* **2007**, *90*, 3099.
(222) Kendrick, E.; Slater, P. R. *Solid State Ionics* **2008**, *179*, 981.
(223) Iwata, T.; Fukuda, K.; Bechade, E.; Masson, O.; Julien, I.; Champion, E.; Thomas, P. *Solid State Ionics* **2008**, *178*, 1523.
(224) Pramana, S. S.; Klooster, W. T.; White, T. J. *J. Solid State Chem.* **2008**, *181*, 1717.
(225) Porras-Vazquez, J. M.; Losilla, E. R.; Leon-Reina, L.; Marrero-Lopez, D.; Aranda, M. A. G. *J. Am. Ceram. Soc.* **2009**, *92*, 1062.
(226) Bonhomme, C.; Beaudet-Savignat, S.; Chartier, T.; Geffroy, P.-M.; Sauvet, A-L *J. Euro. Ceram. Soc.* **2009**, *29*, 1781.
(227) Najib, A.; Sansom, J. E. H.; Tolchard, J. R.; Islam, M. S.; Slater, P. R. *Dalton Trans.* **2004**, *19*, 3106.
(228) Tolchard, J. R.; Islam, M. S.; Slater, P. R. *J. Mater. Chem.* **2003**, *13*, 1956.
(229) Ali, R.; Yashima, M.; Matsushita, Y.; Yoshioka, H.; Okoyama, K.; Izumi, F. *Chem. Mater.* **2008**, *20*, 5203.
(230) Bechade, E.; Masson, O.; Iwata, T.; Julien, I.; Fukuda, K.; Thomas, P.; Champion, E. *Chem. Mater.* **2009**, *21*, 2508.
(231) Masubuchi, Y.; Higuchi, M; Takeda, T.; Kikkawa, S. *Solid State Ionics* **2006**, *177*, 263.
(232) Jones, A; Slater, P. R.; Islam, M. S. *Chem. Mater.* **2008**, *20*, 5055.
(233) Nakayama, S.; Niguchi, M. *J. Mater. Sci. Lett.* **2001**, *20*, 913.
(234) Abram, E. J.; Sinclair, D. C.; West, A. R. *J. Mater. Chem.* **2001**, *11*, 1978.
(235) Shaula, A. L.; Kharton, V. V.; Marques, F. M. B. *J. Solid State Chem.* **2005**, *178*, 2050.
(236) Kendrick, E.; Islam, M. S.; Slater, P. R. *Solid State Ionics* **2007**, *177*, 3411.
(237) Tolchard, J. R.; Slater, P. R.; Islam, M. S. *Adv. Funct. Mater.* **2007**, *17*, 2564.
(238) Yoshioka, H.; Nojiri, Y.; Tanase, S. *Solid State Ionics* **2008**, *179*, 2165.
(239) Kendrick, E.; Islam, M. S.; Slater, P. R. *Chem. Commun* **2008**, 715.
(240) Kendrick, E.; Orera, A.; Slater, P. R. *J. Mater. Chem.* **2009**, *19*, 7955.
(241) Kendrick, E.; Slater, P. R. *Mater. Res. Bull.* **2008**, *43*, 2509.
(242) Rodriguez-Reyna, E.; Fuentes, A. F.; Maczka, M.; Hanuza, J.; Boulahya, K.; Amador, U. *Solid State Sci.* **2006**, *8*, 168.
(243) McFarlane, J.; Barth, S.; Swaffer, M.; Sansom, J. E. H.; Slater, P. R. *Ionics* **2002**, *8*, 149.
(244) Tsipis, E. V.; Kharton, V. V.; Frade, J. R. *Electrochim. Acta* **2007**, *52*, 4428.
(245) Yaremchenko, A. A.; Kharton, V. V.; Bannikov, D. O.; Znosak, D. V.; Frade, J. R.; Cherepanov, V. A. *Solid State Ionics* **2009**, *180*(11−13), 878.
(246) Kendrick, E.; Headspith, D.; Orera, A.; Apperley, D. C.; Smith, R. I.; Francesconi, M. G.; Slater, P. R. *J. Mater. Chem.* **2009**, *19*, 749.
(247) Kuang, X.; Green, M. A.; Niu, H.; Zajdel, P.; Dickinson, C.; Claridge, J. B.; Jantsky, L.; Rosseinsky, M. J. *Nat. Mater.* **2008**, *7*, 498.
(248) Joubert, O.; Magrez, A.; Chesnaud, A.; Caldes, M. T.; Jayaraman, V.; Piffard, Y.; Brohan, L. *Solid State Sci.* **2002**, *4*, 1413.
(249) Martin-Sedeno, M. C.; Losilla, E. R.; Leon-Reina, L.; Bruque, S.; Marrero-Lopez, D.; Nunez, P.; Aranda, M. A. G. *Chem. Mater.* **2004**, *16*, 4960.
(250) Martin-Sedeno, M. C.; Marrero-Lopez, D.; Losilla, E. R.; Leon-Reina, L.; Bruque, S.; Nunez, P.; Aranda, M. A. G. *Chem. Mater.* **2005**, *17*, 5989.
(251) Martin-Sedeno, M. C.; Marrero-Lopez, D.; Losilla, E. R.; Bruque, S.; Nunez, O.; Aranda, M. A. G. *J. Solid State Chem.* **2006**, *179*, 3445.
(252) Kendrick, E.; Russ, M. A.; Slater, P. R. *Solid State Ionics* **2008**, *179*, 819.
(253) Amezawa, K.; Maekawa, H.; Tomii, Y.; Yamamoto, N. *Solid State Ionics* **2001**, *145*, 233.
(254) Kitamura, N.; Amezawa, K.; Tomii, Y.; Yamamoto, N. *Solid State Ionics* **2003**, *162−163*, 161.
(255) Haugsrud, H R.; Norby, T. *Nat. Mater.* **2006**, *56*, 193.
(256) Kuwabara, A.; Haugsrud, R.; Stolen, S.; Norby, T. *Phys. Chem. Chem. Phys.* **2009**, *11*, 5550.
(257) Mokkelbost, T.; Kaus, I.; Hausgrud, R.; Norby, T.; Grande, T.; Einarsrud, M. A. *J. Am. Ceram. Soc.* **2008**, *91*, 879.
(258) Tolchard, J. R.; Lein, H. L.; Grande, T. *J. Eur. Ceram.* **2009**, *29*, 2823.
(259) Schönberger, F.; Kendrick, E.; Islam, M. S.; Slater, P. R. *Solid State Ionics* **2005**, *176*, 2951.
(260) Kendrick, E.; Islam, M. S.; Slater, P. R. *Proc. SOFC IX* **2005**, *2*, 1142.
(261) Kendrick, E.; Kendrick, J.; Knight, K. S.; Islam, M. S.; Slater, P. R. *Nat. Mater.* **2007**, *6*, 871.
(262) Irvine, J. T. S.; Slater, P. R.; Wright, P. A. *Ionics* **1996**, *2*, 213.
(263) Slater, P. R.; Fagg, D. P.; Irvine, J. T. S. *J. Mater. Chem.* **1987**, *7*, 2495.
(264) Slater, P. R.; Irvine, J. T. S. *Solid State Ionics* **1999**, *120*, 125.
(265) Slater, P. R.; Irvine, J. T. S. *Solid State Ionics* **1999**, *124*, 61.
(266) Fu, Q. X.; Tietz, F.; Stover, D. *J. Electrochem. Soc.* **2006**, *153*, D74.
(267) Kendrick, E.; Islam, M. S.; Slater, P. R. *Solid State Ionics* **2005**, *176*, 2975.
(268) Canales-Vasquez, J.; Tao, S. W.; Irvine, J. T. S. *Solid State Ionics* **2003**, *159*, 159.
(269) Canales-Vasquez, J.; Ruiz-Morales, J. C.; Irvine, J. T. S.; Zhou, W. Z. *J. Electrochem. Soc.* **2005**, *152*, A1382.
(270) Ovalle, A.; Ruiz-Morales, J. C.; Canales-Vazquez, J.; Marrero-Lopez, D.; Irvine, J. T. S. *Solid State Ionics* **2006**, *177*, 1997.
(271) Ruiz-Morales, J. C.; Canales-Vazquez, J.; Savaniu, C.; Marrero-Lopez, D.; Zhou, W. Z.; Irvine, J. T. S. *Nature* **2006**, *439*, 568.
(272) Ruis-Morales, J. C.; Canales-Vazquez, J.; Savaniu, C.; Marrero-Lopez, D.; Nunez, P.; Zhou, W. Z.; Irvine, J. T. S. *Phys. Chem. Chem. Phys.* **2007**, *9*, 1821.
(273) Escudero, M. J.; Irvine, J. T. S.; Daza, L. *J. Power Sources* **2009**, *192*, 43.
(274) Hui, S. Q.; Petric, A. *J. Eur. Ceram. Soc.* **2002**, *22*, 1673.
(275) Karczewski, J.; Riegel, B.; Molin, S.; Winiarski, A.; Gazda, M.; Jasinski, P.; Murawski, L.; Kusz, B. *J. Alloys Compounds* **2009**, *473*, 496.
(276) Sauvet, A. L.; Fouletier, J. *J. Power Sources* **2001**, *101*, 259.
(277) Sauvet, A. L.; Irvine, J. T. S. *Solid State Ionics* **2004**, *167*, 1.
(278) Tao, S. W.; Irvine, J. T. S. *Nat. Mater.* **2003**, *2*, 320.
(279) Vernoux, P.; Guillodo, M.; Fouletier, J.; Hammou, A. *Solid State Ionics* **2000**, *135*, 425.
(280) Sfeir, J.; Buffat, P. A.; Mockli, P.; Xanthopoulis, P.; Vasquez, R.; Mathieu, J. J.; Herle, J. V.; Thampi, K. R. *J. Catal.* **2001**, *202*, 229.
(281) Tao, S. W.; Irvine, J. T. S. *J. Electrochem. Soc.* **2004**, *151*, A252.
(282) Raj, E. S.; Kilner, J. A.; Irvine, J. T. S. *Solid State Ionics* **2006**, *177*, 1747.
(283) Kharton, V. V.; Tsipis, E. V.; Marozau, I. P.; Viskup, A. P.; Frade, J. R.; Irvine, J. T. S. *Solid State Ionics* **2007**, *178*, 101.
(284) Liu, J.; Madsen, B. D.; Li, Z. Q.; Barnett, S. A. *Electrochem. Solid State Lett.* **2002**, *5*, A122.
(285) Jiang, S. P.; Ye, Y. M.; He, T. M.; Ho, S. B. *J. Power Sources* **2008**, *185*, 179.
(286) Chen, X. J.; Liu, Q. L.; Chan, S. H.; Brandon, N. P.; Kor, K. A. *J. Electrochem. Soc.* **2007**, *154*, B1206.
(287) Lay, E.; Gauthier, G.; Rosini, S.; Savaniu, C.; Irvine, J. T. S. *Solid State Ionics* **2008**, *179*, 1562.
(288) Tao, S. W.; Irvine, J. T. S. *Solid State Ionics* **2008**, *179*, 725.
(289) Hui, S. Q.; Petric, A. *Solid State Ionics* **2001**, *143*, 275.
(290) Cheng, Z.; Zha, S. W.; Aguilar, L.; Liu, M. L. *Solid State Ionics* **2005**, *176*, 1921.
(291) Aguadero, A.; de la Calle, C.; Alonso, J. A.; Perez-Coll, D.; Escudero, M. J.; Daza, L. *J. Power Sources* **2009**, *192*, 78.
(292) Huang, Y. H.; Dass, R. I.; Xing, Z. L.; Goodenough, J. B. *Science* **2006**, *312*, 254.
(293) Huang, Y. H.; Dass, R. I.; Denyszyn, J. C.; Goodenough, J. B. *J. Electrochem. Soc.* **2006**, *153*, A1266.
(294) Huang, Y. H.; Liang, G.; Croft, M.; Lehtimaki, M.; Karppinen, M.; Goodenough, J. B. *Chem. Mater.* **2009**, *21*, 2319.
(295) Matsuda, Y.; Karppinnen, M.; Yamazaki, Y.; Yamauchi, H. *J. Solid State Chem.* **2009**, *182*, 1713.
(296) Bernuy-Lopez, C.; Allix, M.; Bridges, C. A.; Claridge, J. B.; Rosseinsky, M. J. *Chem. Mater.* **2007**, *19*, 1035.
(297) Marrero-Lopez, D.; Pena-Martinez, J.; Ruiz-Morales, J. C.; Martin-Sedeno, M. C.; Nunez, P. *J. Solid State Chem.* **2009**, *182*, 1027.
(298) Wei, T.; Ji, Y.; Meng, X. W.; Zhang, Y. L. *Electrochem. Commun.* **2008**, *10*, 1369.
(299) Tao, S. W.; Irvine, J. T. S. *J. Solid State Chem.* **2002**, *165*, 12.
(300) Tao, S. W.; Irvine, J. T. S. *J. Electrochem. Soc.* **2004**, *151*, A497.
(301) Deng, Z. Q.; Niu, H. J.; Kuang, X. J.; Allix, M.; Claridge, J. B.; Rosseinsky, M. J. *Chem. Mater.* **2008**, *20*, 6911.